



Published in final edited form as:

*Dev Biol.* 2015 November 1; 407(1): 40–56. doi:10.1016/j.ydbio.2015.08.009.

## ***Wt1* and $\beta$ -catenin cooperatively regulate diaphragm development in the mouse**

Nicole D. Paris<sup>a</sup>, Garry L. Coles<sup>a</sup>, and Kate G. Ackerman<sup>a,b,1</sup>

<sup>a</sup>Department of Biomedical Genetics, University of Rochester School of Medicine and Dentistry, Rochester, NY 14642, USA

<sup>b</sup>Department of Pediatrics, Center for Pediatric Biomedical Research, University of Rochester School of Medicine and Dentistry, Rochester, NY 14642, USA

### **Abstract**

The developing diaphragm consists of various differentiating cell types, many of which are not well characterized during organogenesis. One important but incompletely understood tissue, the diaphragmatic mesothelium, is distinctively present from early stages of development. Congenital Diaphragmatic Hernia (CDH) occurs in humans when diaphragm tissue is lost during development, resulting in high morbidity and mortality postnatally. We utilized a *Wilms Tumor 1* (*Wt1*) mutant mouse model to investigate the involvement of the mesothelium in normal diaphragm signaling and development. Additionally, we developed and characterized a *Wt1<sup>CreERT2</sup>*-driven  $\beta$ -catenin loss-of-function model of CDH after finding that canonical Wnt signaling and  $\beta$ -catenin are reduced in *Wt1* mutant mesothelium. Mice with  $\beta$ -catenin loss or constitutive activation induced in the *Wt1* lineage are only affected when tamoxifen injection occurs between E10.5 and E11.5, revealing a critical time-frame for *Wt1*/ $\beta$ -catenin activity. Conditional  $\beta$ -catenin loss phenocopies the *Wt1* mutant diaphragm defect, while constitutive activation of  $\beta$ -catenin on the *Wt1* mutant background is sufficient to close the diaphragm defect. Proliferation and apoptosis are affected, but primarily these genetic manipulations appear to lead to a change in normal diaphragm differentiation. Our data suggest a fundamental role for mesothelial signaling in proper formation of the diaphragm.

### **Keywords**

Wt1;  $\beta$ -catenin; Congenital Diaphragmatic Hernia; Wnt signaling; Diaphragm development; Mesothelium

---

<sup>1</sup>Corresponding author: Center for Pediatric Biomedical Research, Box 611, University of Rochester School of Medicine and Dentistry, 601 Elmwood Ave, Rochester, NY 14642, USA. Phone: (585) 276-4001, Fax: (585) 276-0232, kate\_ackerman@urmc.rochester.edu.

**Publisher's Disclaimer:** This is a PDF file of an unedited manuscript that has been accepted for publication. As a service to our customers we are providing this early version of the manuscript. The manuscript will undergo copyediting, typesetting, and review of the resulting proof before it is published in its final citable form. Please note that during the production process errors may be discovered which could affect the content, and all legal disclaimers that apply to the journal pertain.

## Introduction

The diaphragm is an essential, and often overlooked, respiratory organ that functions in breathing, esophageal contraction, separation of the body cavities and regulation of fluids in the thoracic and abdominal cavities (Abu-Hijleh et al., 1995; Bordoni and Zanier, 2013; Pickering and Jones, 2002). Congenital Diaphragmatic Hernia (CDH) is a relatively common birth defect occurring in approximately 1 in 3,000 live births, and as many as 1 in 2,000 pregnancies, and is a major source of mortality and morbidity (Greer, 2013; Harrison et al., 1994). CDH is a birth defect affecting more than just the diaphragm, as more often a complex spectrum of defects are present in the heart and lungs. This can be due to primary genetic mechanisms, as well as secondary mechanical issues (Ackerman et al., 2005; Babiuk and Greer, 2002; Chiu, 2014). The most common and most severe types of CDH occur in the posterior and lateral regions, which have historically been grouped as “Bochdalek” hernias (Ackerman et al., 2012; Pober, 2007). In embryonic development, the pleuroperitoneal folds (PPFs), present at E11.5–E12.5 in the mouse, are thought to contribute to a substantial portion of the diaphragm mesenchyme (Greer et al., 2000). It is believed that prior to this event, the septum transversum forms the anterior region, or central tendon, of the diaphragm (Yuan et al., 2003). The mature diaphragm is made up of various tissue types including muscle, tendon, connective tissue, nerve, blood vessels, lymphatics and mesothelium (Ackerman and Greer, 2007; Zhang et al., 2014). Defects in several of these diaphragmatic cell types have been investigated in genetic mouse models of CDH, including connective tissue (Ackerman et al., 2005; Jay et al., 2007; Merrell et al., 2015; You et al., 2005), tendon (Coles and Ackerman, 2013; Domyan et al., 2013; Yuan et al., 2003), and blood vessels (Zhang et al., 2014). Mesothelium and non-muscle mesenchyme are present throughout diaphragm development, but have yet to be fully characterized.

The mesothelium is a mesoderm-derived epithelial-like cell layer important for lubrication of internal organs via secretion of surfactant. Recently, a developmental role has been established for mesothelial cells, as they have been shown to contribute to the mesoderm of organs such as the heart, lungs, liver and gut (Asahina et al., 2011; Que et al., 2008; Wilm et al., 2005; Zhou et al., 2008). In early development, mesothelium is present after gastrulation in the coelomic cavity (Thomas, 1987). Mesothelial cells are able to differentiate into adipocytes, chondrocytes, and osteoblasts; as well as fibroblasts and smooth muscle cells in *in vitro* models, which may reflect their contribution in embryonic development (Batra and Antony, 2014). The cellular characteristics of the mesothelium are uniquely associated with both epithelial and mesenchymal morphology and expression. Due to this feature, both cuboidal and squamous types of mesothelial cells exist, where squamous are thought to be the most differentiated form (Herrick and Mutsaers, 2004). Cuboidal mesothelial cells coating highly mobile organs are biosynthetically active with primary cilia, abundant Golgi, rough endoplasmic reticulum, microvilli, lamellar bodies, basement membrane, cell-cell junctions, and extensive cytoskeletal networks (Bird, 2004). These cellular characteristics are important for tensile strength and flexibility. In the pleural cavity, mature mesothelial cells play a critical role in inflammatory response, fluid homeostasis, and maintenance of the elasticity required for organs to expand during development (Charalampidis et al., 2015). Mesothelial cells at different stages of maturation and with unique gene expression can be

found predominantly on the thoracic surface of the developing diaphragm, while mesothelium on the abdominal side develops at later stages after complete separation of the diaphragm from the liver (Shinohara, 1997). Mesothelial Slit-Robo signaling may be critical to the development of the central tendon of the diaphragm, as proper signaling is necessary to ensure that the anterior diaphragm correctly separates from the liver and maintains its integrity (Domyan et al., 2013; Yuan et al., 2003).

The genetic mechanisms that function in diaphragm development are still largely unknown. Several genes have been implicated in normal diaphragm development and are associated with human CDH, but the extensive study of mouse genetic models is often limited by embryonic lethality (Ackerman et al., 2005; Beurskens et al., 2007; Jay et al., 2006; You et al., 2005). One of these genes, *Wilms Tumor 1 (Wt1)*, was determined to be necessary for diaphragm development in a mouse model of urogenital developmental defects (Kreidberg et al., 1993). Additionally, limited studies of the *Wt1* null embryonic diaphragm identified defects in the posterolateral region, possibly originating from lost PPF tissue early in diaphragm development (Clugston et al., 2006). *Wt1* is a zinc finger transcription factor/tumor suppressor important for organogenesis, which is expressed in the urogenital system as well as by the mesothelium lining the body wall and covering the heart, lungs, diaphragm, and liver beginning at E9.5 (Moore et al., 1998; Rackley et al., 1993). It has been established that *Wt1* is mutated in several complex human diseases such as Denys-Drash, Meacham, and Frasier syndromes, at times presenting with CDH (Antonius et al., 2008; Suri et al., 2007). *Wt1* acts upstream of a variety of genes to regulate numerous processes during development (Wagner et al., 2003). Previous findings in the kidney have identified *Wt1* downstream targets in diverse pathways, including MAP kinase signaling, axon guidance, and Wnt signaling (Kim et al., 2009).

Canonical Wnt signaling is responsible for many cellular processes such as cell proliferation, cell fate specification, and differentiation (Logan and Nusse, 2004). Genes associated with Wnt signaling in the diaphragm have been shown to be preferentially expressed during early organogenesis, and a few Wnt pathway members have been indirectly associated with human CDH (Russell et al., 2012; Wat et al., 2011). A connection between *Wt1* and Wnt signaling has been previously elucidated in the heart, where it has been suggested that *Wt1* acts upstream of  $\beta$ -*Catenin* to regulate epithelial-mesenchymal transition (EMT) (von Gise et al., 2011). *Wt1* binding sites have also been identified and validated in several Wnt pathway members; including *Lef1* in the kidney and posterior taste field of the tongue (Gao et al., 2014; Hartwig et al., 2010). Apart from a role for Wnt signaling in skeletal muscle maturation during late embryogenesis, Wnt has not yet been implicated in the process of diaphragm development (Mathew et al., 2011).

In this study, we propose one mechanism of *Wt1* function in diaphragm development in which canonical Wnt signaling is promoted by targeting  $\beta$ -*catenin*. We show data demonstrating that Wnt signaling in diaphragm development is required during a specific time in a distinct subset of non-muscle cells, which primarily includes mesothelial cells. We have further elucidated the function of *Wt1* as well as developed a new conditional genetic model using the inducible *Wt1<sup>CreERT2</sup>* mouse, which survives until birth. This model expands opportunities for the investigation of developmental mechanisms in the diaphragm

as previous models such as the *Wt1* null mutant only live until E13.5–E14.5 (Clugston et al., 2006; Kreidberg et al., 1993). To our knowledge, we are the first to propose a role for mesothelial signaling in the development of the posterior diaphragm.

## Materials and Methods

### Experimental Mice and Genotyping

All animal studies were approved by the University Committee on Animal Resources at the University of Rochester Medical Center. *R26RlacZ* (JAX: 003309) and *BATgal* reporter mice (JAX: 005317) were purchased from the Jackson laboratory (Maretto et al., 2003; Soriano, 1999). *Axin2<sup>lacZ</sup>* (JAX: 009120), *TOPgal* (JAX: 004623), *Bcat<sup>fx</sup>* (*Ctnnb1<sup>tm2Kem</sup>*; JAX: 004152), and *Bcat<sup>ex3fx</sup>* (*Ctnnb1<sup>tm1Mmt</sup>*; MGI:1858008) mice were provided by Wei Hsu (Department of Biomedical Genetics, University of Rochester, Rochester, NY) (Brault et al., 2001; DasGupta and Fuchs, 1999; Harada et al., 1999; Lustig et al., 2002). These strains were genotyped as described by the Jackson Laboratory.

*Wt1<sup>GFP<sup>Cre</sup></sup>* (JAX: 010911) and *Wt1<sup>CreERT2</sup>* (JAX: 010912) mice were obtained from William T. Pu (Department of Cardiology, Children's Hospital Boston, Boston, NY) and maintained by our lab on the outbred Swiss Webster (CFW) line (Zhou et al., 2008). *Wt1<sup>GFP<sup>Cre</sup></sup>* mice were used to analyze *Wt1* loss for all experiments other than the rescue experiment, where it was necessary to use *Wt1<sup>CreERT2</sup>*. Both strains of mice lack the first coding exon of *Wt1* and were genotyped by Cre PCR (Cre313F- 5'-CCACGACCAAGTGACAGCAATG-3', Cre705R- 5'-TTCGGATCATCAGCTACACCAGAG-3' Eurofins Genomics, annealing temp 60°). To distinguish *Wt1* heterozygous embryos from homozygotes, TaqMan duplex allelic discrimination analysis of yolk sac DNA was carried out to detect Cre copy number compared to control Beta-microglobulin exon sequence. BioRad iQ Supermix buffer was used as well as primers and probes from Biosearch Technologies, listed below. Assays were run at an annealing temperature of 55°.

Cre F Primer	5'-CCGCAGGTGTAGAGAAGGC-3'
Cre R Primer	5'-AACAGGTAGTTATTCGGATCATCAG-3'
BMG F Primer	5'-TTGTCATGTTGGTTGAGAAGCAG-3'
BMG R Primer	5'-TATGAACTCAGGTGGTCAGGTTG-3'
BMG Probe	CAL Fluor Red 610-5'-TGCTGAGCCATACCACTGCCATCTT-3'-BHQ-2
Cre Probe	FAM-5'-ACACCAGAGACGGAAATCCATCGCT-3'-BHQ-1

Where it was necessary to detect GFP, *Wt1<sup>GFP<sup>Cre</sup></sup>* heterozygotes were used as littermate controls because they were phenotypically normal during embryonic development. Homozygous mice (*Wt1<sup>GFP<sup>Cre</sup>/GFP<sup>Cre</sup></sup>*) are denoted as *Wt1* null or mutant given that the Cre is a knock-in construct. In some experiments, *Wt1<sup>GFP<sup>Cre</sup></sup>* mice were bred to *Wt1<sup>CreERT2</sup>* heterozygotes to maintain one copy of GFP for immunofluorescence. These mice were genotyped to differentiate *Wt1<sup>GFP<sup>Cre</sup></sup>* from *Wt1<sup>CreERT2</sup>* alleles with *Wt1* and Cre primers as follows: *Wt1F*- 5'-AGAATCCGCAGGATCGCAGGAG-3', Cre4002R- 5'-GCTTGCATGATCTCCGGTAT-3', annealing temp 60°. Cre-negative embryos were used as a wildtype control unless otherwise indicated. *Wt1<sup>CreERT2/+</sup>;Bcat<sup>fx/+</sup>* (one allele LOF)

embryos were determined to be phenotypically normal, thus  $\beta$ -catenin homozygous loss-of-function embryos were generated.

### Embryo Generation and Histology

Embryos were harvested at E10.5–E15.5, where noon of the day the mucous plug was observed was considered E0.5. For some conditional  $\beta$ -catenin loss-of-function experiments, pups were collected just after birth and dissected for phenotypic analysis. Yolk sacs were removed for DNA extraction. To induce activation of *Wt1<sup>CreERT2</sup>*, 2–2.5 mg of 10 mg/ml tamoxifen (MP Biomedical #156738), dissolved in sesame oil at 37°C, was injected intraperitoneally into pregnant females (Zhou and Pu, 2012). Mice were injected once between E8.5–E12.5. Embryos were fixed overnight at 4°C in 4% paraformaldehyde in PBS for sectioning or 10% formalin for gross dissection. Paraffin sections were cut at 7  $\mu$ m and stained with hematoxylin and eosin (H&E) using standard methods for histological analysis. For histological staining of elastin fibers, Hart's Stain was used and sections were counterstained with eosin or tartrazine. Unless otherwise noted, each experiment was conducted in embryos from three separate litters for a given age.

### X-gal Staining

To detect  $\beta$ -galactosidase expression in the *LacZ* reporter mice, whole embryos at E10.5–E11.5 or partially dissected embryos at E12.5–E14.5 were fixed in a 0.2% glutaraldehyde, 5 mM EGTA, 2 mM MgCl<sub>2</sub> solution overnight at 4°C. Embryos were then permeabilized with a solution of 100 mM sodium phosphate buffer pH 7.3, 0.02% NP40, 0.01–0.05% sodium deoxycholate, and 2 mM MgCl<sub>2</sub> for at least 30 minutes. Embryos were then incubated in a staining solution of 5 mM potassium ferricyanide, 5 mM potassium ferrocyanide, 50 mg X-gal (Lab Scientific), and permeabilization buffer overnight at room temperature (Nagy et al., 2007). Tissue was post-fixed in 10% formalin, or 4% paraformaldehyde for immunostaining. Paraffin sections (10  $\mu$ m) were then counterstained with Nuclear Fast Red. For frozen sections, embryos at E11.5–E13.5 were fixed as described above, washed in 30% sucrose, and embedded in OTC. Cryosections (10  $\mu$ m) were post-fixed with 0.2% glutaraldehyde prior to X-gal staining.

### Immunostaining

Paraffin tissue sections were prepared for immunofluorescence or immunohistochemistry following standard methods. Antigen retrieval was performed in a Food Steamer (Oster #5711) in 10 mM sodium citrate pH 6.0, 0.05% Tween 20 or 10 mM Tris, 1 mM EDTA pH 9.0, 0.05% Tween 20 buffer for 20 minutes (after preheating 20 minutes). For some antibodies, more extensive antigen retrieval in a pressure cooker at 120°C for 20 minutes was necessary. Primary antibodies used were as follows: rabbit anti-Wilms Tumor 1 (1:500; Abcam; ab89901), mouse anti-BrdU (1:300; BD Biosciences; #347580), rabbit anti-Cleaved Caspase 3 (1:500; Cell Signaling; #9661), mouse anti-Myosin (MF20) (1:100; DSHB; AB\_2147781), mouse anti-Active  $\beta$ -catenin (anti-ABC) (1:500; Millipore; 05-665), chicken anti-GFP (1:300; Abcam; ab13970), goat anti-Podocalyxin (1:200; R&D Systems; AF1556), mouse anti-Collagen1a1 (1:250; Sigma; SAB1402151), rabbit anti-TCF4 (1:300; Cell Signaling; C48H11), rabbit anti-PDGFR $\alpha$  (1:500; Cell Signaling; D1E1E), mouse anti-

Twist1 (1:250; Santa Cruz; sc-81417), rabbit anti-Sox9 (1:1,000; Millipore; AB5535), mouse anti-N-Cadherin (1:500; BD Biosciences; 610920), mouse anti-P-Cadherin (1:10; Abcam; ab75442), and mouse anti-E-Cadherin (1:500; BD Biosciences; 610182). A second Wt1 antibody (mouse anti-human) was needed for co-labeling with antibodies raised in rabbit (1:20–1:100; ThermoScientific; 6F-H2). Secondary antibodies for immunofluorescence were purchased from Life Technologies and were applied at 1:200 dilution with Hoechst stain (1:1,000; ThermoScientific). For IHC, biotinylated goat anti-rabbit or goat anti-mouse (1:300; Vector; BA-1000 or BA-9200, respectively) were used. Streptavidin-Peroxidase polymer (Sigma S2438) was applied at 1:500 for one hour prior to application of DAB substrate (Abcam ab64238). For IHC of Active  $\beta$ -catenin, the Vector M.O.M. immunodetection kit (BMK-2202) was used. To amplify IHC signal of low background-producing antibodies such as Twist1 and TCF4, the peroxidase Vector ImmPRESS Reagent (MP-7402 or MP-7401) was used. The MF20 (Myosin) antibody developed by Fischman, D.A. at Weill Cornell Medical College was obtained from the Developmental Studies Hybridoma Bank, created by the NICHD of the NIH and maintained at The University of Iowa, Department of Biology, Iowa City, IA 5224.

### Cell Proliferation and Cell Death Analysis

Pregnant females were injected intraperitoneally with 20 mg/ml bromo-deoxyuridine (BrdU) (Sigma B5002) at 50–100 $\mu$ g per one gram mouse weight one hour before embryo harvest for cell proliferation experiments. Embryos were fixed in 4% paraformaldehyde and processed in paraffin for immunofluorescence of tissue sections. *Wt1<sup>GFP</sup>Cre* and *Wt1<sup>CreERT2</sup>* mice were crossed to generate *Wt1* null and heterozygous embryos, maintaining one copy of GFP in both genotypes. *Wt1<sup>GFP</sup>Cre/CreERT2* embryos were compared to their respective *Wt1<sup>GFP</sup>Cre/+* littermates. *Wt1<sup>CreERT2/+</sup>; Bcat<sup>fx/fx</sup>* and *Wt1<sup>CreERT2/+</sup>; Bcat<sup>ex3fx/+</sup>* embryos were harvested after tamoxifen injection at E10.5 and compared to their respective *Wt1<sup>+/+</sup>* littermates. Co-immunofluorescence for Wt1 (or GFP) and BrdU was performed on comparable sections in four different regions (one per slide) of the left and right diaphragm at E12.5. The number of Wt1/GFP, BrdU positive cells, and double positive cells in the mesothelial layer (any cell lying adjacent to the pleural cavity) of the posterior diaphragm was counted, along with total number of mesothelial cells, in at least three sections in each region. Cell death analysis was carried out on different sections of the same E12.5 embryos by immunofluorescent staining of Cleaved Caspase 3 on four slides per embryo. Cleaved Caspase 3-positive cells in the entire posterior diaphragm were counted and compared to the total number of posterior cells.

These experiments were performed in at least three different sets of littermates for each genotype. ImageJ software was utilized for cell counting and merging fluorescent images (Schneider et al., 2012). Cell counts were recorded as a percent of total Hoechst-positive cells. Mutant cell counts were normalized to the control for visualization of the relative rate of cell proliferation/cell death. Statistical significance was determined using a two-tailed *t*-test assuming unequal variance, where  $P < 0.05$  was considered significant and mutants were compared to their respective littermate control (not one another). Data was plotted using Standard Error of Mean. *P* values were reported as calculated by *t*-test, but significance was also validated by One-Way ANOVA.

## Imaging and Microscopy

Leica MZ 12-5 and Leica DM 5500B microscopes were used to image samples. A Leica MC 170HD camera was used to capture color images and a Leica DFC 365FX camera to capture fluorescent images. Respectively, LAS V4.3 and LAS AF software was used to acquire images. Image editing and addition of scale bars was done using ImageJ software.

## Results

### **Wt1 contributes to the diaphragm mesothelium and mesenchyme in an age-dependent manner**

*Wt1* expression in organogenesis is typically restricted to either the mesenchyme (kidney and gonad) or the mesothelium (visceral organs and body cavity lining). *Wt1* is expressed in the non-muscle mesenchyme of the primordial diaphragm (pleuroperitoneal folds) (Clugston and Greer, 2007), but specific localization of *Wt1* expression during maturation of the embryonic diaphragm is unknown. For this reason, we examined *Wt1* expression in wildtype mouse embryos during the entire process of diaphragm development (E11.5 to E15.5). Unlike other *Wt1*-expressing organs, we determined that the diaphragm actively expresses *Wt1* in both mesothelium and a subset of mesenchymal cells throughout diaphragm organogenesis, though *Wt1* protein remains heavily localized to the mesothelium during this time (Fig. 1A, C, G, and J). To further characterize *Wt1*-positive mesenchymal cells, we utilized antibodies targeting the non-muscle mesenchyme and the muscle fibers. To identify a new non-muscle mesenchymal marker, expression analysis was conducted to determine the localization of the transcription factor *Twist-related protein 1* (*Twist1*) in the diaphragm. *Twist1*, a mesoderm-determining factor important for specification and differentiation during mouse development, is expressed in many different tissues, including *Wt1*-derived cells in the heart (Qin et al., 2012; Zhou et al., 2011). We found that the *Wt1*-positive diaphragmatic mesenchyme largely corresponds to *Twist1*-positive undifferentiated mesenchyme (~70% overlap at E13.5), and these cells do not overlap with skeletal muscle markers (Supplementary Fig. 1A–D). The presence of *Wt1* in specific diaphragmatic cell types during a critical period of development suggests that it plays a distinct role in the formation of a functional diaphragm.

The temporal contribution of *Wt1*-expressing cells to the diaphragm was examined to investigate *Wt1* function and to characterize conditional mouse tools for further study of diaphragm development. Tamoxifen inducible *Wt1<sup>CreERT2</sup>* mice were determined to be most effective for this study, as *Wt1<sup>GFP<sup>Cre</sup></sup>* mice are non-inducible and wide recombination of *R26RlacZ* (due to ubiquitous early expression) precluded specific labeling of cells in the diaphragm (unpublished results). *Wt1<sup>CreERT2</sup>* mice have been successfully utilized to lineage trace mesothelial cells in other tissues such as the epicardium of the heart (Zhou et al., 2008). Although this mouse model is ideal for investigating potential epithelial-mesenchymal transition (EMT) mechanisms in other organs, the presence of *Wt1* expression in both mesothelial and mesenchymal diaphragmatic cells limits analysis in this tissue. Despite this limitation, the *Wt1<sup>CreERT2</sup>* mouse line is a very effective tool for mapping *Wt1*-expressing cells during development in a time-dependent manner. *Wt1<sup>CreERT2</sup>; R26RlacZ* embryos, injected with tamoxifen at E8.5 to induce reporter activity, were analyzed at

E11.5–E13.5 (Fig. 1B, D and H). Analysis of *Wt1* lineage labeling induced at this time rarely showed staining as robust as age-matched *Wt1* antibody staining. To rule out incomplete penetration of X-gal staining buffer, the specificity of the fate map staining pattern was verified by examining X-gal stained cryosections of PPF tissue at E11.5 (Supplementary Fig. 1I). We also established that whole mount X-gal staining was consistent with previously reported labeling of the *Wt1* lineage in the developing heart and lungs (Supplementary Fig. 1F) (Que et al., 2008; Zhou et al., 2008). We then induced *R26RlacZ* reporter expression in the developing diaphragm at ages E9.5 and E10.5 to analyze the pattern of *Wt1* contribution at E12.5 (Fig. 1D–F) and E13.5 (Fig. 1H and I). When *Wt1* lineage labeling occurs at E10.5 (Fig. 1F), rather than E8.5–E9.5, there is a noticeable shift in the *lacZ* staining pattern, revealing a heavier contribution to the posterior diaphragm evident as early as one day after Cre activation (Supplementary Fig. 1J and K). These findings were validated by *Wt1* antibody staining of X-gal stained sections at E12.5, which showed a significantly increased overlap of *Wt1* contribution and protein in the posterior diaphragm of embryos injected at E10.5 (Supplementary Fig. 1G and H). The age-specific pattern of *Wt1* contribution seen after induction at E10.5 coincides with a time of significant tissue growth and migration, as observed by others through morphological examination of the developing primordial diaphragm, implicating *Wt1* in functions necessary for this process (Merrell et al., 2015). By E15.5, *Wt1* protein localization in the mature diaphragm becomes more restricted to the mesothelium (Fig. 1J). In contrast, *Wt1* fate-mapped cells were detected in the entire diaphragmatic mesothelial surface and were highly concentrated in the body wall connection of the posterior diaphragm (Fig. 1K and L). Interestingly, this site is also a region that is vulnerable to diaphragmatic defects. These findings suggest that there are dynamic changes in the pattern of *Wt1* contribution and expression in the mesothelium and mesenchyme throughout diaphragm development that have not previously been appreciated. Further investigation is still needed to elucidate the mechanisms in which *Wt1* functions in diaphragm development.

### Normal $\beta$ -catenin expression in the diaphragm mesothelium is regulated by *Wt1*

*Wt1* target genes involved in diaphragm function have not yet been identified. Wnt is one of several signaling pathways with preferential gene expression during early diaphragm development that also falls downstream of *Wt1* signaling in other organs (Kim et al., 2009; Russell et al., 2012). By co-immunofluorescence, we found that  $\beta$ -catenin is present in a subset of *Wt1*-expressing mesothelial cells at both early and later stages of normal diaphragm development, in addition to expected expression in the muscle fibers (Fig. 2A and B) (Kuroda et al., 2013). To determine if  $\beta$ -catenin is affected by the loss of *Wt1*, homozygous null embryos were generated using the *Wt1*<sup>GFPCre</sup> mouse line and analyzed by antibody staining. Notably, mesothelial protein levels of both active (Fig. 2C and D) and total (Supplementary Fig. 2E and F)  $\beta$ -catenin were significantly reduced in *Wt1* mutant diaphragms, with no alteration of expression in muscle fibers. Since  $\beta$ -catenin has additional roles independent of Wnt signaling, further studies were needed to verify that canonical Wnt signaling is altered in the *Wt1* mutant diaphragm.

For subsequent analysis of canonical Wnt signaling in the diaphragm, we utilized the *Axin2*<sup>lacZ</sup> reporter mouse, a knock-in construct reflecting the endogenous expression of



downstream target *Axin2* upon activation of the Wnt pathway. Whole mount analysis of this reporter in the wildtype diaphragm at E12.5 revealed more concentrated staining in the late PPF (the future posterior diaphragm) compared to the expanding anterior diaphragm; where individual, stained mesothelial cells are visible above the unstained liver (Fig. 2E). These findings suggest that *Axin2<sup>lacZ</sup>* faithfully recapitulates mesothelial  $\beta$ -catenin localization visualized in tissue sections of the developing diaphragm. In X-gal stained embryos generated from *Axin2<sup>lacZ</sup>;Wt1<sup>GFP</sup>Cre* heterozygous matings, mesothelial staining was drastically reduced in the *Wt1* null posterior diaphragm at E11.5 (Fig. 2F–I), similar to the specific reduction of  $\beta$ -catenin protein that was observed. Since Wnt reporter mice have never been characterized in the diaphragm, we also examined *BATgal* and *TOPgal* transgenic mice at E11.5. These mice carry multiple TCF/LEF binding sites (targeted by active Wnt) artificially driven by ubiquitous promoters. We determined that these reporters did not reflect both mesothelial and muscular antibody staining of  $\beta$ -catenin, making the resulting X-gal staining experiments in the *Wt1* mutant diaphragm inconclusive (Supplementary Fig. 2A–D). All three types of Wnt reporter mice have shown variability depending on the tissue context, for instance in the lung, where direct comparison has been carried out (Al Alam et al., 2011). Since  $\beta$ -catenin expression has not been previously characterized in the developing diaphragm, additional cell types were evaluated to determine the entire localization. Connective tissue cells that express *Transcription factor 4 (TCF4)* (Mathew et al., 2011), a gene whose protein product forms a complex with  $\beta$ -catenin during Wnt signaling in other tissues (van de Wetering et al., 2002), were a potential source of  $\beta$ -catenin expression in the diaphragm. Given this association, we assayed TCF4/Active  $\beta$ -catenin overlap in the diaphragm by co-immunofluorescence. Very few TCF4-positive mesothelial cells are double positive for Active  $\beta$ -catenin, therefore these cells do not account for the activation of Wnt signaling seen throughout the diaphragm mesothelium in *Axin2<sup>lacZ</sup>* embryos (Supplementary Fig. 2G and H). TCF4 also does not substantially overlap with markers of *Wt1*-positive non-muscle mesenchyme in the posterior diaphragm such as *Twist1*, indicating that TCF4-positive cells would not be expected to be directly affected in *Wt1* mouse models (Supplementary Fig. 1E). Thus far, non-muscle  $\beta$ -catenin appears to be exclusively associated with and regulated by *Wt1* in the diaphragm mesothelium. We next wanted to test whether  $\beta$ -catenin, in addition to *Wt1*, plays a role in diaphragm signaling necessary for proper development.

### **$\beta$ -catenin in *Wt1*-expressing cells is necessary for proper diaphragm development**

To determine if the loss of  $\beta$ -catenin is functionally significant, a conditional loss-of-function model using the inducible *Wt1<sup>CreERT2</sup>* line was developed. First, comprehensive phenotypic analysis of *Wt1* null mature diaphragms was performed in order to have detailed records for comparison when examining  $\beta$ -catenin deficient diaphragms. From 14 litters of *Wt1<sup>GFP</sup>Cre* heterozygous matings harvested at E15.5, 38 of 124 (30.6%) total embryos screened were genotyped as *Wt1<sup>GFP</sup>Cre* homozygous (null) mutants, and 21% of embryos had apparent intrauterine demise. All intact mutants were examined, and 100% displayed bilateral posterior diaphragmatic hernia (Fig. 3A and B) with some variation in severity. By histological analysis of *Wt1* null sagittal sections, posterior diaphragmatic hernia with lung herniation into the abdominal cavity could be easily observed at E14.5 (Fig. 3G and H). We also noted that central tendon patterning was disrupted, similar to a mouse model we

previously reported (Fig. 3B) (Coles and Ackerman, 2013). We expected that if  $\beta$ -catenin is important in *Wt1*-expressing cells, then a similar phenotype would be observed when it is lost from cells in the *Wt1* lineage.

*Wt1*-induced  $\beta$ -catenin loss-of-function (*Wt1*<sup>CreERT2/+</sup>;*Bcat*<sup>fx/fx</sup>) embryos harvested from dams injected at E10.5 died postnatally, in contrast to the *Wt1* null embryonic lethality that occurs at E13.5–E15.5. Analysis of embryos collected at Postnatal Day 0 (P0) revealed complete loss of the posterior diaphragm in all  $\beta$ -catenin mutants examined (Fig. 3C and D), which is the same region affected in the *Wt1* mutant. The central tendon patterning appeared unaffected in these mice, in contrast to *Wt1* null mice. By evaluation of gross morphology, there was obvious bilateral pulmonary hypoplasia and displacement of the heart associated with liver herniation into the thoracic cavity, similar to phenotypes associated with CDH in humans (Fig. 3E, F and I–L). As expected, these pups were born gasping and cyanotic and were unable to expand their lungs properly. The distal pulmonary air spaces are collapsed when viewed by histology (Fig. 3K and L). Similar findings have been reported in other CDH mouse models, for instance in *Robo1*;<sup>2</sup> mutants where mispositioning of the stomach in the thoracic cavity is observed (Domyan et al., 2013). The *Wt1* mutant also has complex lung defects, including rounded, abnormally fused lung lobes, which have been previously characterized (Cano et al., 2013). With *Wt1*-specific  $\beta$ -catenin loss, a normal number of malformed, but appropriately separated, lung lobes were observed. Further characterization of the *Wt1*<sup>CreERT2</sup>;*Bcat*<sup>fx</sup> embryos was needed to verify tissue-specific  $\beta$ -catenin loss and to determine if the effect seen was age dependent.

As we anticipated, *Wt1*<sup>CreERT2</sup>;*Bcat*<sup>fx</sup> diaphragm mesothelium experienced a nearly complete loss of  $\beta$ -catenin not observed in the muscle cells (Fig. 3M and N). Infrequent  $\beta$ -catenin-positive cells that remained were *Wt1*-negative, consistent with a lack of recombination in a small subset of mesothelial cells due to the expression pattern of *Wt1*. The mesothelium retained normal levels of *Wt1* protein, however. This persistence of *Wt1* expression after  $\beta$ -catenin loss places  $\beta$ -catenin downstream of *Wt1*. Additionally, we did not detect loss of  $\beta$ -catenin from the lung mesothelium, possibly a result of the specific timing of recombination.  $\beta$ -catenin deletion at E10.5 was crucial in order to observe a diaphragmatic hernia phenotype. Tamoxifen injections occurring before E10.5 (Supplementary Fig. 3) or after E11.5 (unpublished data) were unable to induce a diaphragmatic phenotype. Active  $\beta$ -catenin could still be detected by immunofluorescence in some diaphragm mesothelial cells of *Wt1*<sup>CreERT2/+</sup>;*Bcat*<sup>fx/fx</sup> embryos induced prior to E10.5 as well. These experiments have identified a requirement for  $\beta$ -catenin in the diaphragm mesothelium during a specific time in development. Gain-of-function experiments would determine if  $\beta$ -catenin is sufficient to drive processes in the developing diaphragm as well as further characterize the relationship between *Wt1* and  $\beta$ -catenin.

### **Wt1-driven constitutive activation of $\beta$ -catenin is sufficient to close *Wt1* null diaphragm defects**

Excision of exon 3 of  $\beta$ -catenin via Cre-lox mouse tools renders the protein incapable of being degraded normally in the cytoplasm, allowing excessive signaling of the Wnt pathway to take place (Harada et al., 1999). Manipulation of  $\beta$ -catenin to drive expression of this

stabilized form in other systems has resulted in expansion of progenitor cells with inhibition of tissue differentiation in a variety of contexts, including the diaphragm muscle (Liu et al., 2012; Mirando et al., 2010). Upregulation of Wnt signaling is also associated with human diseases involving abnormal proliferation and differentiation such as pulmonary fibrosis and cancer (Moon et al., 2004). We hypothesized that  $\beta$ -catenin stabilization in the diaphragm could promote similar processes involving tissue expansion to prevent or reverse the formation of a diaphragm defect in *Wt1* null embryos. The inducible *Wt1<sup>CreERT2</sup>* mice were crossed to the  $\beta$ -catenin exon 3-floxed (*Bcat<sup>ex3fx</sup>*) mouse line and double heterozygotes were mated to generate litters of both wildtype and *Wt1* null embryos with  $\beta$ -catenin activation. When  $\beta$ -catenin was constitutively activated in the *Wt1* lineage by tamoxifen injection at E10.5 (Fig. 4A–D), we did, in fact, observe excessive tissue growth with the formation of mesothelial-associated nodules in diaphragms with wildtype *Wt1* expression. Furthermore, constitutively active  $\beta$ -catenin on the *Wt1* null background in these litters was able to fill the diaphragm defect with unorganized mesenchymal tissue (based on histological appearance) by E13.5. The embryonic lethality observed in the *Wt1* mutant mice was not affected by activation of  $\beta$ -catenin, suggesting that diaphragmatic *Wt1*/Wnt signaling is distinct from that of the heart. Notably, in *Wt1<sup>CreERT2</sup>; Bcat<sup>ex3fx</sup>* litters collected one day prior to complete closure of the diaphragm defect (E12.5), the process of mesenchymal expansion in double mutant diaphragms was occurring, but the defect had not yet fully closed (Fig. 4J). Similar to *Wt1*-induced loss-of-function, E10.5 was the optimal time for induction of recombination that resulted in a phenotype. There was no effect on the diaphragm with injection at E8.5, though injection at E9.5 did result in a mild phenotype (formation of small nodules) (Supplementary Fig. 3). When injected later, at E11.5,  $\beta$ -catenin stabilization did drive some mesenchymal overgrowth, however *Wt1* null diaphragms were still left with an open defect. It was important to further characterize the changes in gene expression resulting from *Wt1*-specific  $\beta$ -catenin stabilization in order to identify the mechanisms contributing to the observed phenotype.

To confirm activation of  $\beta$ -catenin, *Wt1<sup>CreERT2</sup>; Bcat<sup>ex3fx</sup>* embryos were assayed with the *Axin2<sup>lacZ</sup>* reporter (Fig. 4E and F), revealing a substantial upregulation of canonical Wnt signaling in diaphragm mesothelium at E11.5. Immunofluorescence revealed massive accumulation of total  $\beta$ -catenin protein (Fig. 4G–J) in regions of the mesothelium and mesenchyme of the posterior diaphragm at E12.5. The active  $\beta$ -catenin antibody, which targets dephosphorylated Ser37/Thr41 residues in exon 3, no longer labels most mesothelial cells adjacent to nodules (Fig. 4K), given that the stabilized  $\beta$ -catenin has had exon 3 removed. We were also able to visualize the two mesothelial surfaces of the *Wt1* null diaphragm defect merging at E13.5 (Fig. 4L) following stabilization of  $\beta$ -catenin. This was observed by co-immunofluorescence of mesothelial-expressed Podocalyxin (PCLP1) (Onitsuka et al., 2010) and Collagen1a1 (Col1a1), a component of the basement membrane of mesothelial cells (Rennard et al., 1984). Collagen1a1 also displayed expanded localization adjacent to the fusing mesothelium, possibly indicative of enhanced activity of these cells, since normal expression is restricted to the basal lamina. Interestingly, both  $\beta$ -catenin conditional gain-of-function and loss-of-function embryos are affected on the right, but not the left, side of the diaphragm if injected too late in the day on E10.5 (~E10.75) (unpublished results). This reflects previous work suggesting that the diaphragm develops

asymmetrically, since left-sided defects occur earlier than right-sided ones in the nitrofen rat model of CDH (Allan and Greer, 1997; Mayer et al., 2011). Our work identifies an important time window for  $\beta$ -catenin function around E10.5 in mouse embryonic diaphragm development. Since we observed loss and gain of tissue with  $\beta$ -catenin deletion and stabilization, respectively, we subsequently wondered how cellular processes may be altered in these models to drive their particular phenotypes.

### Cell proliferation and apoptosis are regulated by *Wt1* and $\beta$ -catenin signaling in the posterior diaphragm

Mouse models of CDH have been proposed to develop diaphragm defects through a variety of different defective cellular mechanisms, supporting the idea that there may be several possible ways for a specific type of diaphragm defect to arise. For example, the diaphragms of *Gata4* heterozygous mice underwent increased apoptosis, but had normal cell proliferation (Jay et al., 2007), whereas nitrofen-exposed embryos were shown to have decreased cell proliferation with no change in cell death (Clugston et al., 2010). Thus, we chose to assay both cell proliferation (by BrdU incorporation) and cell death (by Cleaved Caspase 3 staining) in all three mouse models discussed above. Pregnant females were injected intraperitoneally with bromo-deoxyuridine (BrdU) one hour prior to harvesting embryos at E12.5, to remain consistent with the work done in the nitrofen model as well as our own work (Coles and Ackerman, 2013). E12.5 was the ideal age to assay, since tamoxifen kinetics may prevent full recombination until up to a day following injection (at E10.5) in the conditional models (Nakamura et al., 2006) and by E13.5, diaphragm defects have already formed. In sagittal sections, diaphragm mesothelial cells labeled by co-immunofluorescence for *Wt1* (or surrogate marker GFP in *Wt1* null tissue), BrdU, or both, were counted and recorded as a percentage of all Hoechst-positive mesothelial cells in the posterior diaphragm (Fig. 5A–C), given that this is the region where the defects occur. The mesothelium was specifically assayed as this is the location of *Wt1* and  $\beta$ -catenin overlap and therefore this cell type is possibly the source of these diaphragm defects. Interestingly, we found that in all three models (*Wt1* null, *Bcat* LOF, and *Bcat* GOF), there was a significant decrease (20–30%) in mesothelial *Wt1* (or GFP)-positive cells relative to the normalized control. The number of cells that had incorporated BrdU had decreased significantly (~20%) in  $\beta$ -catenin loss-of-function diaphragm mesothelium, but had increased significantly (~60%) in the gain-of-function model. Similar significant changes were seen in the percentage of *Wt1*/BrdU double positive cells. No significant change was seen in the subset of cells that had incorporated BrdU, but were *Wt1*-negative. An exception was the gain-of-function mesothelium which experienced a significant increase in this cell population similar to what was seen for all BrdU-positive and double labeled cells. Representative *Wt1*/BrdU immunostained sections of  $\beta$ -catenin loss-of-function (Fig. 5B and C), *Wt1* null, and  $\beta$ -catenin gain-of-function (Supplementary Fig. 4) embryos reflect these findings. No significant changes could be detected in total cell number in the posterior mesothelium (Supplementary Fig. 4J), which suggests loss of *Wt1* (or GFP) expression rather than complete loss of a subset of *Wt1*-positive cells. Cells in the entire posterior diaphragm were also counted (Supplementary Fig. 4I) in case there were additional defects in proliferation from non-cell-autonomous signaling or mesenchymal *Wt1* expression, but no significant differences could be detected. This result could also be due to the fact that *Wt1*

and BrdU-positive cells only make up about 20% of the posterior diaphragm, and the larger number of single Hoechst-positive cells could dilute any real differences that may be occurring. Since the BrdU incorporation in only a portion of *Wt1* (or GFP)-expressing cells was affected by *Wt1* loss or  $\beta$ -*catenin* manipulation, additional cellular processes could also be affected.

*Wt1* null,  $\beta$ -*catenin* loss-of-function, and  $\beta$ -*catenin* gain-of-function embryonic sections were assayed for cell death by immunofluorescence of Cleaved Caspase 3 at E12.5 (Fig. 5D–F). Cells from the entire posterior diaphragm were counted in this case, however, due to the localization and low number of caspase-positive cells. We saw a significant change in all three models, where *Wt1* and  $\beta$ -*catenin* loss led to an approximately three-fold increase in cells undergoing apoptosis. Stabilization of  $\beta$ -*catenin* had the reverse effect, decreasing cell death by over 50%, which normally occurs at very low levels in the diaphragm (Clugston et al., 2010). In representative Cleaved Caspase 3 immunostained sections of  $\beta$ -*catenin* loss-of-function (Fig. 5E and F), *Wt1* null, and  $\beta$ -*catenin* gain-of-function mutant embryos (Supplementary Fig. 4), excessive Caspase 3 staining is generally detected in the region of the posterior diaphragm closest to the connection to the body wall, where diaphragm defects later form. Further immunofluorescent analysis of Caspase 3 localization was carried out in  $\beta$ -*catenin* loss-of-function diaphragms with a different *Wt1* antibody raised in mouse (Supplementary Fig. 4K). Though cell death was present in scattered mesenchymal cells, a subset of the Caspase 3-positive cells near the body wall connection appeared to associate with *Wt1*-positive cells, but were not double positive. We also observed infrequent Caspase 3 staining in the mesothelium of the posterior diaphragm, but overall, mesenchymal staining was much more prevalent. These data suggest that *Wt1* and  $\beta$ -*catenin* in the diaphragm mesothelium regulate cell proliferation by cell-autonomous signaling and apoptosis by non-cell-autonomous signaling. With both of these cellular processes affected, it seemed that normal differentiation of the diaphragm may also be affected by perturbation of *Wt1* or  $\beta$ -*catenin*.

### **Stabilization of $\beta$ -catenin in the *Wt1* lineage of the diaphragm drives the accumulation of undifferentiated non-muscle mesenchyme**

Since it is difficult to identify a defective mechanism in the lost diaphragm tissue of the *Wt1* null and  $\beta$ -*catenin* loss-of-function models, we believed that it would be beneficial to use the  $\beta$ -*catenin* gain-of-function model to identify genes or processes that are affected in this system in order to enhance our understanding of CDH models. Since *Wt1* has previously been implicated in the process of EMT in other tissues, we hypothesized that enhanced transition of the mesothelial cells into mesenchymal cells due to constitutively active  $\beta$ -*catenin* could be responsible for diaphragmatic nodule formation. *Wt1*<sup>CreERT2</sup>;*Bcat*<sup>ex3fx</sup> mice were crossed to the *R26RlacZ* reporter (Fig. 6A) and induced at E10.5 to label *Wt1*-derived cells in the diaphragm nodules. The resulting fate map showed that at least 80% of cells in the nodules were *lacZ* positive. These findings indicated that either the *Wt1*-expressing non-muscle mesenchyme was being amplified or that new mesenchymal cells were being derived from *Wt1*-expressing mesothelium, since only mesothelial *Wt1* protein is detected in association with the nodules (Fig. 4K).

We then assessed the integrity of the basement membrane of mesothelial cells adjacent to nodules, since loss of these extracellular matrix (ECM) components can be a hallmark of EMT, at least in epithelial cells (Zeisberg and Neilson, 2009). Collagen types I, III, and IV, laminin, fibronectin, and elastin are just a few proteins of the ECM associated with mesothelial cells in culture (Rennard et al., 1984). Elastin fibers lying beneath the mesothelial cells were visualized histologically by Hart's stain (Fig. 6B and C). The darkly stained fibers appeared to be continuous around the mesothelial surface of the nodule (Fig. 6C), except where the nodules were pushed into adjacent tissues such as the liver (Fig. 6B). By eosin counterstaining, intact collagen fibers of the submesothelial layer and within the unaffected diaphragm mesenchyme were apparent. This well-formed connective tissue prevented infiltration of the accumulating nodule mesenchyme, which is often characteristic of malignant neoplasia (Mutsaers, 2002). By immunofluorescence, Collagen1a1 in the basement membrane was lost from some mesothelial cells at the nodule periphery (Fig. 6D). The disruption of the mesothelial basement membrane is only one hallmark of EMT, however, and could simply be a result of mechanical stress on these ECM components from rapid tissue growth in the mesenchyme. A further characteristic of epithelial or mesothelial cells undergoing EMT is a reduction in cell-surface cadherin expression (Zeisberg and Neilson, 2009).

In contrast to the “cadherin switching” characteristically undergone by epithelial cells actively undergoing EMT, normal mesothelial cells may express all of the three main cadherins (E-Cadherin, N-Cadherin, and P-Cadherin), with a preference for N-Cadherin (Simsir et al., 1999). When these cell-surface proteins were assayed in  $\beta$ -catenin gain-of-function diaphragm nodules (Fig. 6J–L), no loss was detected, though differential expression in the lung (Fig. 6J'–L') did serve as a positive control. Of the known acquired mesenchymal markers of EMT, we were limited to proteins specifically localized in the diaphragm and not widely expressed (since the mesothelium is derived from mesenchyme). Twist1 was a prime candidate, though it is also expressed during normal diaphragm development (most likely initiating mesenchymal gene programs), which is a confounding factor for assaying EMT. By immunofluorescence (Fig. 6E), it was clear that almost the entire area of mesenchymal overgrowth was Twist1 positive. Additionally, a lack of mesenchymal co-labeling with Wt1 was observed, which is unique given that extensive co-labeling is normally seen in the wildtype diaphragm at this age (Supplementary Fig. 1C). Other markers of undifferentiated mesenchyme were established in the diaphragm, and were also present in and around the accumulating mesenchymal nodules, such as Sox9 (SRY (sex determining region Y)-box 9) (Fig. 6F) and Pdgfra (Platelet-derived growth factor receptor alpha) (Fig. 6G) (Furuyama et al., 2011; Uezumi et al., 2014). Labeling of several differentiated cell types by muscle marker Myosin (Fig. 6G) and connective tissue marker TCF4 (Fig. 6H) indicated that these cells were absent from the bulk of the nodule mesenchyme. Additionally, unlike the results of the cell death assay at E12.5 where apoptosis was reduced, at E13.5 we began to see Cleaved Caspase 3-positive cells in the mesenchyme of the diaphragm nodules (Fig. 6I). This suggests that the nodules are not able to sustain themselves due to the specific time requirement for active  $\beta$ -catenin. Taken together, these data do not clearly support an induction of EMT in the mesothelium due to  $\beta$ -catenin overactivation, since the mesothelial structure generally remains intact and cadherin localization in the diaphragm is unchanged.

We can conclude, however, that constitutive activation of  $\beta$ -catenin in the mesothelium results in the accumulation of undifferentiated mesenchyme in localized regions of the diaphragm by E13.5.

### **Wt1 maintains mesothelial integrity while both Wt1 and $\beta$ -catenin are required for appropriate differentiation of the diaphragm mesenchyme**

Previous work established that there is a defect in lung mesothelial structure of the *Wt1* mutant mouse, in addition to commonly observed defects in EMT-associated signaling (Cano et al., 2013; Karki et al., 2014). When the diaphragm mesothelial cell morphology of the *Wt1* null embryos was analyzed by histology (Fig. 7E–H), the cells appeared morphologically to be more cuboidal and lacked ECM components such as elastin fibers, consistent with an immature phenotype. Similarly, a *Slit3* deficient mouse model of CDH also displayed decreased presence of elastin at E13.5 in the central tendon mesothelium (Yuan et al., 2003). Following the same analysis,  $\beta$ -catenin loss-of-function diaphragm mesothelium appeared normal in structure and maturity (Fig. 7M and N). The non-muscle mesenchyme was assayed for appropriate differentiation, given the amplification of undifferentiated mesenchyme markers in the  $\beta$ -catenin gain-of-function diaphragms. Twist1-positive mesenchyme labeled by immunohistochemistry was significantly reduced in the posterior diaphragms of *Wt1* null (Fig. 7C and D) and  $\beta$ -catenin loss-of-function (Fig. 7K and L) embryos. Other differentiated cell type markers, such as Myosin, were reduced in *Wt1* null posterior diaphragms (Fig. 7A and B) but not in the  $\beta$ -catenin loss-of-function diaphragms (Fig. 7I and J). Additionally, Podocalyxin, a cell surface protein present in the mesothelium, was not changed in either mutant model (Fig. 7 I, J, O and P). Therefore, our data suggest that *Wt1* functions through  $\beta$ -catenin signaling to specifically regulate *Twist1*, which drives the appropriate differentiation of the diaphragm mesenchyme.  $\beta$ -catenin is not required for all aspects of *Wt1* signaling, as there are defects in mesothelial maturation that appear to be unique to the *Wt1* null model. Our findings identify a more extensive role for *Wt1* function in the developing diaphragm that most likely targets additional downstream genes other than  $\beta$ -catenin.

## **Discussion**

### **Conditional perturbation of $\beta$ -catenin signaling downstream of Wt1 is necessary and sufficient to drive tissue-specific diaphragm phenotypes at a precise time in development**

Embryonic lethality has prohibited prior investigation of the mechanisms underlying the formation of *Wt1* null diaphragm defects. One of several possible *Wt1* downstream signaling pathways, Wnt signaling, has also been unexplored in the diaphragm, largely due to the need to perform site and time specific manipulation of the pathway to avoid severe, global developmental defects. We were able to utilize the inducible *Wt1<sup>CreERT2</sup>* mouse tool along with  $\beta$ -catenin floxed mice to conditionally target a subset of diaphragm cells without extensive recombination in other vital organs such as the heart.  $\beta$ -catenin loss-of-function and gain-of-function studies in the inducible *Wt1*-driven system placed  $\beta$ -catenin downstream of *Wt1*. Evidence for this relationship includes the phenocopy of the  $\beta$ -catenin loss-of-function and the *Wt1* null diaphragm defects (in which mesothelial  $\beta$ -catenin is drastically reduced), the ability of constitutive activation of  $\beta$ -catenin to rescue the *Wt1* null

diaphragm defect, and the overall retention of *Wt1* expression in the mesothelium of diaphragms with loss of  $\beta$ -*catenin*. Though the stabilization of  $\beta$ -*catenin* resulted in closure of the diaphragmatic defect, the tissue was not fully restored to a normal state. This tissue was highly undifferentiated, perhaps due to an inappropriately high level of Wnt activation or due to other pathways *Wt1* may be targeting. Our findings reinforce studies associating *Wt1* and  $\beta$ -*catenin* in cardiac development (von Gise et al., 2011) and provide additional evidence for this relationship with the analysis of experiments conditionally activating  $\beta$ -*catenin*.

The timing of signaling events during diaphragm development has remained elusive without the ability to conditionally target developing diaphragm cells with an inducible mouse tool. We chose to test the inducible *Wt1<sup>CreERT2</sup>* mouse line, as it has proven effective when used for in depth studies of the heart (Zhou et al., 2008). Our analysis of *Wt1* contribution using *Wt1<sup>CreERT2</sup>* and *R26RlacZ* indicated that this mouse line would provide a specific, robust Cre-recombinase tool for probing mechanisms of diaphragm development. Based on our findings from fate mapping and  $\beta$ -*catenin* manipulation experiments, E10.5–E11.5 was identified as a critical time window for essential Wnt signaling during diaphragm development. As suspected based on the dynamic shift of *Wt1* contribution during early organogenesis,  $\beta$ -*catenin* manipulation induced earlier than E10.5 was unable to create a diaphragm phenotype. Unfortunately, we cannot definitively eliminate the possibility that  $\beta$ -*catenin* has a role before this time because the developmental timing of *Wt1* expression driving the inducible Cre does not appear to promote complete recombination in the mesothelium earlier than E10.5. The particular timing that we were able to establish supports a key model for CDH in mice, in which diaphragm development at the PPF stage (E11.5) is extremely vulnerable to any defects in basic cellular processes that may then act as a driving force for the formation of diaphragm phenotypes (Clugston et al., 2006; Jay et al., 2007; Merrell et al., 2015; You et al., 2005).

### **Mesothelial signaling in the diaphragm may be necessary to regulate the proper differentiation of the posterior diaphragm mesenchyme**

Previous work carried out on the mesothelium in other organs, such as the lung, identified a model in which mesothelial signaling, apart from epithelial-mesenchymal transition (EMT), is necessary for proper mesenchymal gene expression (Yin et al., 2011). As early as E11.5, the wildtype diaphragm has a distinctive mesothelial layer with cell-type specific gene expression as well as unique protein localization at the cell surface and in the basement membrane, the latter of which cannot be maintained when *Wt1* is lost. These mesothelial characteristics, as well as additional features of maturation, persist beyond embryonic development and continue to be maintained in the adult diaphragm, making it critical that they are established correctly. Though  $\beta$ -*catenin* was not specifically required for the formation of mature mesothelium, it was evident that it is responsible for appropriate signal transduction in this tissue. Analysis of *Wt1* (or GFP) immunofluorescent labeling in the genetically manipulated mesothelial cells designated functions for both  $\beta$ -*catenin* and *Wt1* in the maintenance of the *Wt1*-positive cell population. With loss of either gene, a reduction in this subset of posterior diaphragmatic mesothelial cells was observed without a detectable change in total cell number. We hypothesize that mesothelial cells co-expressing *Wt1* and  $\beta$ -



*catenin* have a specific gene expression profile that provides a signaling function distinct from the adjacent *Wt1*-negative mesothelium. Perhaps the establishment and maintenance of the correct proportion of these two cell populations in early diaphragm development is necessary for proper morphogenesis. Additionally, it is unclear whether changes in mesothelial cell proliferation are partly responsible for the diaphragm phenotypes observed, although our findings are similar to those reported in the PPF of the nitrofen-induced rat model of CDH (Clugston et al., 2010). Similarity between the deficiencies observed in the *Wt1*-positive subpopulation of cells in *Wt1* null and  $\beta$ -*catenin* loss-of-function diaphragmatic mesothelium suggests that cell-autonomous signaling of these genes may form a feedback loop that is necessary to maintain proper expression of other diaphragm mesothelial genes that are required for these cells to mature appropriately.

In addition to the mesothelial defects that result from *Wt1* and  $\beta$ -*catenin* deletion, we also identified specific deficiencies in the diaphragm non-muscle mesenchymal cells triggered by increased cell death and failure to maintain the *Twist1*-positive cell population. The apparent inability to maintain *Twist1* expression is consistent with work demonstrating that *Twist1* expression (as well as EMT) is defective in *Wt1* knockout embryonic stem cells (Martínez-Estrada et al., 2010). Reduction of *Twist1* localization in mesenchymal cells of the posterior diaphragm is also significant because *Twist1* is an established downstream target of Wnt signaling (Reinhold et al., 2006). To gain additional knowledge about the similarities in the mutant phenotypes, we were able to identify inappropriately activated mechanisms of diaphragm development in a  $\beta$ -*catenin* gain-of-function model, where amplified cell populations could be readily identified. Using this tool, *Wt1*-derived *Twist1* positive mesenchymal cells accumulated uncontrollably when  $\beta$ -*catenin* activation occurred in the PPF-specific time window (E10.5–E11.5). We propose that the posterior diaphragm defects in our loss-of-function models arise primarily due to failed induction of a mesenchymal differentiation program by *Twist1* in the non-muscle mesenchymal cells. This is suspected based upon the larger proportion of dysfunctional mesenchymal cells (compared to mesothelium), which may compromise the structural integrity of the posterior diaphragm. Our data suggest that the diaphragm mesothelium functions to promote both cell-autonomous signaling driving mesothelial gene expression and non-cell-autonomous signaling that regulates mesenchymal *Twist1* expression, contributing to proper organogenesis. Many phenotypic characteristics are shared between the two mutant models, but several differences, mentioned above, could be a result of either the specific functions of *Wt1* and  $\beta$ -*catenin* in the diaphragm or the conditional targeting of  $\beta$ -*catenin* in this system. Following the comparison of specific changes in normal protein localization in the diaphragms of these genetic mouse models, the phenotypes of *Wt1* and conditional  $\beta$ -*catenin* mutant mice were assessed, and we were able to develop a model for the regulation of diaphragm development by *Wt1*/ $\beta$ -*catenin* signaling (Fig. 8).

### **Development of a tissue-specific genetic mouse tool to model the pathogenesis of human CDH**

Germline deletion of CDH candidate genes in mice often results in embryonic lethality in mid-gestation, limiting the ability to translate studies to postnatal disease mechanisms of human CDH. We have developed an inducible conditional mutant model in the mouse that is

able to survive until birth due to time-specific deletion of  $\beta$ -catenin in *Wt1*-derived cells. The characterization of diaphragmatic mesothelial cells has been a focus of our studies, due to the prominent expression of *Wt1* in this tissue, however, mesothelial defects could be more definitively explored with an inducible Cre mouse that specifically targets the mesothelium of the diaphragm. It remains unclear which gene promoter would drive ideal mesothelial-specific recombination during the critical PPF-period of diaphragm development (E11.5–E12.5). For example, *Mesothelin* would be an excellent candidate to drive mesothelium-specific Cre-recombinase, however studies in the liver and lung have determined that this gene is not expressed until later organogenesis (Dixit et al., 2013; Onitsuka et al., 2010). Alternatively, *Podocalyxin* (*PCLP1*) expression was detected in early mesothelial cells coating the liver in these studies, and we confirmed that it was also present in diaphragm mesothelium as early as E11.5 (unpublished data). Unfortunately, simultaneous expression in vasculature precludes the use of a *PCLP1*-Cre mouse for mesothelial-specific studies. This expression pattern is a common limiting factor indicative of early mesothelial gene functions in multiple mesenchymal lineages. Nevertheless, the development of an inducible *PCLP1*-driven mouse tool could allow for further detailed studies of the immature diaphragm mesothelium.

We have described a valuable genetic system to target the mouse diaphragm consistently without severely affecting the heart or otherwise causing intrauterine demise. Knowledge of *Wt1* function in the diaphragm has been expanded by our ability to manipulate the genes *Wt1* and  $\beta$ -catenin simultaneously utilizing tissue-specific Cre-lox mouse tools. Further studies analyzing the cardiopulmonary phenotype of  $\beta$ -catenin loss-of-function mice could pair gene signaling changes in the diaphragm with CDH-associated defects in these important organ systems, as these tissues may not be directly targeted by the specific timing and localization of the *Wt1*<sup>CreERT2</sup> mouse tool. We have established a possible role for diaphragmatic mesothelial cells in all mouse models of CDH, given that many key genes in addition to *Wt1* and  $\beta$ -catenin can be detected in this cell layer.

Although deficiencies in the mesothelium and the canonical Wnt signaling pathway generate a CDH phenotype in mice, their implication in human CDH has not been proven. Essential genes involved in the Wnt signaling pathway may play a role in human CDH pathogenesis, although cytogenetic data and significant heterogeneity in the population suggest that human genetic abnormalities in this pathway may result in more phenotypic variation than in the mouse (Pober, 2008; Wat et al., 2011). Thus, the mouse may not be an entirely accurate disease model. The relationship between Wnt signaling and human CDH, as well as the functional role of the human diaphragmatic mesothelium, will need to be further explored. It is also possible that there are additional roles for *Wt1* in human diaphragm development that have not yet been identified through the investigation of *Wt1* mutations associated with complex and syndromic CDH (Antonius et al., 2008; Suri et al., 2007). Ultimately, this work and future studies in the mouse will advance the understanding of the dynamics of diaphragm development and the signaling deficiencies which may contribute to the pathogenesis of CDH in humans.

## Supplementary Material

Refer to Web version on PubMed Central for supplementary material.

## Acknowledgments

This work was supported by National Institutes of Health Grant R01 HL085459 to K.G.A. We would like to thank Laurel Baglia for critical reading of the manuscript and technical assistance as well as Lei Xu for technical advice, Helene McMurray for statistical advice, and Nian Zhang for technical assistance and for supplying the total  $\beta$ -catenin antibody. We additionally thank Wei Hsu and William T. Pu for providing mouse reagents.

## References

- Abu-Hijleh MF, Habbal OA, Moqattash ST. The role of the diaphragm in lymphatic absorption from the peritoneal cavity. *J Anat.* 1995; 186:453–467. [PubMed: 7559120]
- Ackerman KG, Greer JJ. Development of the diaphragm and genetic mouse models of diaphragmatic defects. *Am J Med Genet Part C Semin Med Genet.* 2007; 145:109–116.10.1002/ajmg.c.30128 [PubMed: 17436296]
- Ackerman KG, Herron BJ, Vargas SO, Huang H, Tevosian SG, Kochilas L, Rao C, Pober BR, Babiuk RP, Epstein Ja, Greer JJ, Beier DR. Fog2 is required for normal diaphragm and lung development in mice and humans. *PLoS Genet.* 2005; 1:0058–0065.10.1371/journal.pgen.0010010
- Ackerman KG, Vargas SO, Wilson JA, Jennings RW, Kozakewich HPW, Pober BR. Congenital Diaphragmatic Defects: Proposal for a New Classification Based on Observations in 234 Patients. *Pediatr Dev Pathol.* 2012; 15:265–274.10.2350/11-05-1041-0a.1 [PubMed: 22257294]
- Al Alam D, Green M, Tabatabai Irani R, Parsa S, Danopoulos S, Sala FG, Branch J, El Agha E, Tiozzo C, Voswinkel R, Jesudason EC, Warburton D, Bellusci S. Contrasting expression of canonical wnt signaling reporters TOPGAL, BATGAL and Axin2 LacZ during murine lung development and repair. *PLoS One.* 2011; 6:e23139.10.1371/journal.pone.0023139 [PubMed: 21858009]
- Allan DW, Greer JJ. Pathogenesis of nitrofen-induced congenital diaphragmatic hernia in fetal rats. *J Appl Physiol.* 1997; 83:338–347. [PubMed: 9262424]
- Antonius T, Van Bon B, Eggink A, Van Der Burgt I, Noordam K, Van Heijst A. Denys-Drash syndrome and congenital diaphragmatic hernia: Another case with the 1097G > A(Arg366His) mutation. *Am J Med Genet Part A.* 2008; 146:496–499.10.1002/ajmg.a.32168 [PubMed: 18203154]
- Asahina K, Zhou B, Pu WT, Tsukamoto H. Septum transversum-derived mesothelium gives rise to hepatic stellate cells and perivascular mesenchymal cells in developing mouse liver. *Hepatology.* 2011; 53:983–995.10.1002/hep.24119 [PubMed: 21294146]
- Babiuk RP, Greer JJ. Diaphragm defects occur in a CDH hernia model independently of myogenesis and lung formation. *Am J Physiol Lung Cell Mol Physiol.* 2002; 283:L1310–L1314.10.1152/ajplung.00257.2002 [PubMed: 12388344]
- Batra H, Antony VB. The pleural mesothelium in development and disease. *Front Physiol.* 2014; 5:284.10.3389/fphys.2014.00284 [PubMed: 25136318]
- Beurskens N, Klaassens M, Rottier R, De Klein A, Tibboel D. Linking animal models to human congenital diaphragmatic hernia. *Birth Defects Res Part A - Clin Mol Teratol.* 2007; 79:565–572.10.1002/bdra.20370 [PubMed: 17469205]
- Bird SD. Mesothelial primary cilia of peritoneal and other serosal surfaces. *Cell Biol Int.* 2004; 28:151–159.10.1016/j.cellbi.2003.11.010 [PubMed: 14984761]
- Bordoni B, Zanier E. Anatomic connections of the diaphragm: Influence of respiration on the body system. *J Multidiscip Healthc.* 2013; 6:281–291.10.2147/JMDH.S45443 [PubMed: 23940419]
- Brault V, Moore R, Kutsch S, Ishibashi M, Rowitch DH, McMahon aP, Sommer L, Boussadia O, Kemler R. Inactivation of the beta-catenin gene by Wnt1-Cre-mediated deletion results in dramatic brain malformation and failure of craniofacial development. *Development.* 2001; 128:1253–1264. [PubMed: 11262227]

- Cano E, Carmona R, Muñoz-Chápuli R. Wt1-expressing progenitors contribute to multiple tissues in the developing lung. *Am J Physiol Lung Cell Mol Physiol*. 2013; 305:L322–32.10.1152/ajplung.00424.2012 [PubMed: 23812634]
- Charalampidis C, Youroukou A, Lazaridis G, Baka S, Mpoukovinas I, Karavasilis V, Kioumis I, Pitsiou G, Papaiwannou A, Karavergou A, Tsakiridis K, Katsikogiannis N, Sarika E, Kapanidis K, Sakkas L, Korantzis I, Lampaki S, Zarogoulidis K, Zarogoulidis P. Physiology of the pleural space. *J Thorac Dis*. 2015; 7:S33–S37.10.3978/j.issn.2072-1439.2014.12.48 [PubMed: 25774305]
- Chiu PPL. New Insights into Congenital Diaphragmatic Hernia – A Surgeon’s Introduction to CDH Animal Models. *Front Pediatr*. 2014; 2:36.10.3389/fped.2014.00036 [PubMed: 24809040]
- Clugston RD, Greer JJ. Diaphragm development and congenital diaphragmatic hernia. *Semin Pediatr Surg*. 2007; 16:94–100.10.1053/j.sempedsurg.2007.01.004 [PubMed: 17462561]
- Clugston RD, Klattig J, Englert C, Clagett-Dame M, Martinovic J, Benachi A, Greer JJ. Teratogen-induced, dietary and genetic models of congenital diaphragmatic hernia share a common mechanism of pathogenesis. *Am J Pathol*. 2006; 169:1541–1549.10.2353/ajpath.2006.060445 [PubMed: 17071579]
- Clugston RD, Zhang W, Greer JJ. Early development of the primordial mammalian diaphragm and cellular mechanisms of nitrofen-induced congenital diaphragmatic hernia. *Birth Defects Res Part A - Clin Mol Teratol*. 2010; 88:15–24.10.1002/bdra.20613 [PubMed: 19711422]
- Coles GL, Ackerman KG. Kif7 is required for the patterning and differentiation of the diaphragm in a model of syndromic congenital diaphragmatic hernia. *Proc Natl Acad Sci U S A*. 2013; 110:E1898–E1905.10.1073/pnas.1222797110 [PubMed: 23650387]
- DasGupta R, Fuchs E. Multiple roles for activated LEF/TCF transcription complexes during hair follicle development and differentiation. *Dev*. 1999; 126:4557–4568.
- Dixit R, Ai X, Fine A. Derivation of lung mesenchymal lineages from the fetal mesothelium requires hedgehog signaling for mesothelial cell entry. *Development*. 2013; 140:4398–4406.10.1242/dev.098079 [PubMed: 24130328]
- Domyan ET, Branchfield K, Gibson Da, Naiche La, Lewandoski M, Tessier-Lavigne M, Ma L, Sun X. Roundabout Receptors Are Critical for Foregut Separation from the Body Wall. *Dev Cell*. 2013; 24:52–63.10.1016/j.devcel.2012.11.018 [PubMed: 23328398]
- Furuyama K, Kawaguchi Y, Akiyama H, Horiguchi M, Kodama S, Kuhara T, Hosokawa S, Elbahrawy A, Soeda T, Koizumi M, Masui T, Kawaguchi M, Takaori K, Doi R, Nishi E, Kakinoki R, Deng JM, Behringer RR, Nakamura T, Uemoto S. Continuous cell supply from a Sox9-expressing progenitor zone in adult liver, exocrine pancreas and intestine. *Nat Genet*. 2011; 43:34–41.10.1038/ng.722 [PubMed: 21113154]
- Gao Y, Toska E, Denmon D, Roberts SGE, Medler KF. WT1 regulates the development of the posterior taste field. *Development*. 2014; 141:2271–2278.10.1242/dev.105676 [PubMed: 24803588]
- Greer JJ. Current concepts on the pathogenesis and etiology of congenital diaphragmatic hernia. *Respir Physiol Neurobiol*. 2013; 189:232–40.10.1016/j.resp.2013.04.015 [PubMed: 23665522]
- Greer JJ, Cote D, Allan DW, Zhang W, Babiuk RP, Ly L, Lemke RP, Bagnall K. Structure of the primordial diaphragm and defects associated with nitrofen-induced CDH. *Journal of applied physiology* (Bethesda, Md: 1985). 2000
- Harada N, Tamai Y, Ishikawa TO, Sauer B, Takaku K, Oshima M, Taketo MM. Intestinal polyposis in mice with a dominant stable mutation of the  $\beta$ -catenin gene. *EMBO Journal*. 1999; 18:21.5931
- Harrison MR, Adzick NS, Estes JM, Howell LJ. A prospective study of the outcome for fetuses with diaphragmatic hernia. *JAMA*. 1994; 271:382–384.10.1001/jama.1994.03510290064038 [PubMed: 8054005]
- Hartwig S, Ho J, Pandey P, Macisaac K, Taglienti M, Xiang M, Alterovitz G, Ramoni M, Fraenkel E, Kreidberg Ja. Genomic characterization of Wilms’ tumor suppressor 1 targets in nephron progenitor cells during kidney development. *Development*. 2010; 137:1189–1203.10.1242/dev.045732 [PubMed: 20215353]
- Herrick SE, Mutsaers SE. Mesothelial progenitor cells and their potential in tissue engineering. *Int J Biochem Cell Biol*. 2004; 36:621–642.10.1016/j.biocel.2003.11.002 [PubMed: 15010328]

- Jay PY, Bielinska M, Erlich JM, Mannisto S, Pu WT, Heikinheimo M, Wilson DB. Impaired mesenchymal cell function in Gata4 mutant mice leads to diaphragmatic hernias and primary lung defects. *Dev Biol.* 2007; 301:602–614.10.1016/j.ydbio.2006.09.050 [PubMed: 17069789]
- Karki S, Surolia R, Hock TD, Guroji P, Zolak JS, Duggal R, Ye T, Thannickal VJ, Antony VB. Wilms' tumor 1 (Wt1) regulates pleural mesothelial cell plasticity and transition into myofibroblasts in idiopathic pulmonary fibrosis. *FASEB J.* 2014; 28:1122–1131.10.1096/fj.13-236828 [PubMed: 24265486]
- Kim MKH, McGarry TJ, Ó Broin P, Flatow JM, Golden AAJ, Licht JD. An integrated genome screen identifies the Wnt signaling pathway as a major target of WT1. *Proc Natl Acad Sci U S A.* 2009; 106:11154–11159.10.1073/pnas.0901591106 [PubMed: 19549856]
- Kreidberg J, Sariola H, Loring JM, Maeda M, Pelletier J, Housman D, Jaenisch R. WT-1 is required for early kidney development. *Cell.* 1993; 74:679–691.10.1016/0092-8674(93)90515-R [PubMed: 8395349]
- Kuroda K, Kuang S, Taketo MM, Rudnicki MA. Canonical Wnt signaling induces BMP-4 to specify slow myofibrogenesis of fetal myoblasts. *Skelet Muscle.* 2013; 3:5.10.1186/2044-5040-3-5 [PubMed: 23497616]
- Liu Y, Sugiura Y, Wu F, Mi W, Taketo MM, Cannon S, Carroll T, Lin W. B-Catenin stabilization in skeletal muscles, but not in motor neurons, leads to aberrant motor innervation of the muscle during neuromuscular development in mice. *Dev Biol.* 2012; 366:255–267.10.1016/j.ydbio.2012.04.003 [PubMed: 22537499]
- Logan CY, Nusse R. The Wnt signaling pathway in development and disease. *Annu Rev Cell Dev Biol.* 2004; 20:781–810.10.1146/annurev.cellbio.20.010403.113126 [PubMed: 15473860]
- Lustig B, Jerchow B, Sachs M, Weiler S, Pietsch T, Karsten U, van de Wetering M, Clevers H, Schlag PM, Birchmeier W, Behrens J. Negative feedback loop of Wnt signaling through upregulation of conductin/axin2 in colorectal and liver tumors. *Mol Cell Biol.* 2002; 22:1184–1193.10.1128/MCB.22.4.1184-1193.2002 [PubMed: 11809809]
- Maretto S, Cordenonsi M, Dupont S, Braghetta P, Broccoli V, Hassan AB, Volpin D, Bressan GM, Piccolo S. Mapping Wnt/ $\beta$ -catenin signaling during mouse development and in colorectal tumors. *Proc Natl Acad Sci U S A.* 2003; 100:3299–3304.10.1073/pnas.0434590100 [PubMed: 12626757]
- Martínez-Estrada OM, Lettice La, Essafi A, Guadix JA, Slight J, Velecela V, Hall E, Reichmann J, Devenney PS, Hohenstein P, Hosen N, Hill RE, Muñoz-Chapulí R, Hastie ND. Wt1 is required for cardiovascular progenitor cell formation through transcriptional control of Snail and E-cadherin. *Nat Genet.* 2010; 42:89–93.10.1038/ng.494 [PubMed: 20023660]
- Mathew SJ, Hansen JM, Merrell AJ, Murphy MM, Lawson Ja, Hutcheson Da, Hansen MS, Angus-Hill M, Kardon G. Connective tissue fibroblasts and Tcf4 regulate myogenesis. *Development.* 2011; 138:371–384.10.1242/dev.057463 [PubMed: 21177349]
- Mayer S, Metzger R, Kluth D. The embryology of the diaphragm. *Semin Pediatr Surg.* 2011; 20:161–169.10.1053/j.sempedsurg.2011.03.006 [PubMed: 21708336]
- Merrell AJ, Ellis BJ, Fox ZD, Lawson JA, Weiss JA, Kardon G. Muscle connective tissue controls development of the diaphragm and is a source of congenital diaphragmatic hernias. *Nat Genet.* 2015; 47:496–504. [PubMed: 25807280]
- Mirando AJ, Maruyama T, Fu J, Yu HMI, Hsu W.  $\beta$ -catenin/cyclin D1 mediated development of suture mesenchyme in calvarial morphogenesis. *BMC Dev Biol.* 2010; 10:116.10.1186/1471-213X-10-116 [PubMed: 21108844]
- Moon RT, Kohn AD, De Ferrari GV, Kaykas A. WNT and beta-catenin signalling: diseases and therapies. *Nat Rev Genet.* 2004; 5:691–701.10.1038/nrg1427 [PubMed: 15372092]
- Moore AW, Schedl A, McInnes L, Doyle M, Hecksher-Sorensen J, Hastie ND. YAC transgenic analysis reveals Wilms' Tumour 1 gene activity in the proliferating coelomic epithelium, developing diaphragm and limb. *Mech Dev.* 1998; 79:169–184.10.1016/S0925-4773(98)00188-9 [PubMed: 10349631]
- Mutsaers SE. Mesothelial cells: Their structure, function and role in serosal repair. *Respirology.* 2002; 7:171–191.10.1046/j.1440-1843.2002.00404.x [PubMed: 12153683]
- Nagy A, Gertsenstein M, Vintersten K, Behringer R. Staining Whole Mouse Embryos for  $\beta$ -Galactosidase (lacZ) Activity. *CSH Protoc.* 2007; 2007.pdb.prot4725. 10.1101/pdb.prot4725

- Nakamura E, Nguyen MT, Mackem S. Kinetics of tamoxifen-regulated Cre activity in mice using a cartilage-specific CreERT to assay temporal activity windows along the proximodistal limb skeleton. *Dev Dyn*. 2006; 235:2603–2612.10.1002/dvdy.20892 [PubMed: 16894608]
- Onitsuka I, Tanaka M, Miyajima A. Characterization and Functional Analyses of Hepatic Mesothelial Cells in Mouse Liver Development. *Gastroenterology*. 2010; 138:1525–1535. e6.10.1053/j.gastro.2009.12.059 [PubMed: 20080099]
- Pickering M, Jones JFX. The diaphragm: Two physiological muscles in one. *J Anat*. 2002; 201:305–312.10.1046/j.1469-7580.2002.00095.x [PubMed: 12430954]
- Pober BR. Genetic aspects of human congenital diaphragmatic hernia. *Clin Genet*. 2008; 74:1–15. [PubMed: 18510546]
- Pober BR. Overview of epidemiology, genetics, birth defects, and chromosome abnormalities associated with CDH. *Am J Med Genet Part C Semin Med Genet*. 2007; 145:158–171.10.1002/ajmg.c.30126 [PubMed: 17436298]
- Qin Q, Xu Y, He T, Qin C, Xu J. Normal and disease-related biological functions of Twist1 and underlying molecular mechanisms. *Cell Res*. 2012; 22:90–106.10.1038/cr.2011.144 [PubMed: 21876555]
- Que J, Wilm B, Hasegawa H, Wang F, Bader D, Hogan BLM. Mesothelium contributes to vascular smooth muscle and mesenchyme during lung development. *Proc Natl Acad Sci U S A*. 2008; 105:16626–16630.10.1073/pnas.0808649105 [PubMed: 18922767]
- Rackley RR, Flenniken aM, Kuriyan NP, Kessler PM, Stoler MH, Williams BR. Expression of the Wilms' tumor suppressor gene WT1 during mouse embryogenesis. *Cell Growth Differ*. 1993; 4:1023–1031. [PubMed: 8117616]
- Reinhold MI, Kapadia RM, Liao Z, Naski MC. The Wnt-inducible transcription factor Twist1 inhibits chondrogenesis. *J Biol Chem*. 2006; 281:1381–1388.10.1074/jbc.M504875200 [PubMed: 16293629]
- Rennard SI, Jaurand MC, Bignon J, Kawanami O, Ferrans VJ, Davidson J, Crystal RG. Role of pleural mesothelial cells in the production of the submesothelial connective tissue matrix of lung. *Am Rev Respir Dis*. 1984; 130:267–274. [PubMed: 6465680]
- Russell MK, Longoni M, Wells J, Maalouf FI, Tracy aa, Loscertales M, Ackerman KG, Pober BR, Lage K, Bult CJ, Donahoe PK. Congenital diaphragmatic hernia candidate genes derived from embryonic transcriptomes. *Proc Natl Acad Sci*. 2012; 109:2978–2983.10.1073/pnas.1121621109 [PubMed: 22315423]
- Schneider CA, Rasband WS, Eliceiri KW. NIH Image to ImageJ: 25 years of image analysis. *Nat Meth*. 2012; 9:671–675.
- Shinohara H. Distribution of lymphatic stomata on the pleural surface of the thoracic cavity and the surface topography of the pleural mesothelium in the golden hamster. *Anat Rec*. 1997; 249:16–23.10.1002/(SICI)1097-0185(199709)249:1<16::AID-AR3>3.0.CO;2-D [PubMed: 9294645]
- Simsir A, Fetsch P, Mehta D, Zakowski M, Abati A. E-cadherin, N-cadherin, and calretinin in pleural effusions: The good, the bad, the worthless. *Diagn Cytopathol*. 1999; 20:125–130.10.1002/(SICI)1097-0339(199903)20:3<125::AID-DC3>3.0.CO;2-V [PubMed: 10086235]
- Soriano P. Generalized lacZ expression with the ROSA26 Cre reporter strain. *Nat Genet*. 1999; 21:70–71.10.1038/5007 [PubMed: 9916792]
- Suri M, Kelehan P, O'Neill D, Vadeyar S, Grant J, Ahmed SF, Tolmie J, McCann E, Lam W, Smith S, FitzPatrick D, Hastie ND, Reardon W. WT1 mutations in Meacham syndrome suggest a coelomic mesothelial origin of the cardiac and diaphragmatic malformations. *Am J Med Genet Part A*. 2007; 143:2312–2320.10.1002/ajmg.a.31924 [PubMed: 17853480]
- Thomas, NW. Embryology and Structure of the Mesothelium. In: Jones, JSP., editor. *Pathology of the Mesothelium*. Springer; London: 1987. p. 1-13.
- Uezumi A, Ikemoto-Uezumi M, Tsuchida K. Roles of nonmyogenic mesenchymal progenitors in pathogenesis and regeneration of skeletal muscle. *Front Physiol*. 2014 Feb.5:68.10.3389/fphys.2014.00068 [PubMed: 24605102]
- Van de Wetering M, Sancho E, Verweij C, de Lau W, Oving I, Hurlstone A, van der Horn K, Battle E, Coudreuse D, Haramis AP, Tjon-Pon-Fong M, Moerer P, van den Born M, Soete G, Pals S, Eilers M, Medema R, Clevers H. The  $\beta$ -Catenin/TCF-4 Complex Imposes a Crypt Progenitor Phenotype

- on Colorectal Cancer Cells. *Cell*. 2002; 111:241–250. [http://dx.doi.org/10.1016/S0092-8674\(02\)01014-0](http://dx.doi.org/10.1016/S0092-8674(02)01014-0). [PubMed: 12408868]
- Von Gise A, Zhou B, Honor LB, Ma Q, Petryk A, Pu WT. Wt1 regulates epicardial epithelial to mesenchymal transition through beta-catenin and retinoic acid signaling pathways. *Dev Biol*. 2011; 356:421–431. [10.1016/j.ydbio.2011.05.668](https://doi.org/10.1016/j.ydbio.2011.05.668). WT1 [PubMed: 21663736]
- Wagner KD, Wagner N, Schedl A. The complex life of WT1. *J Cell Sci*. 2003; 116:1653–1658. [10.1242/jcs.00405](https://doi.org/10.1242/jcs.00405) [PubMed: 12665546]
- Wat MJ, Veenma D, Hogue J, Holder AM, Yu Z, Wat JJ, Hanchard N, Shchelochkov Oa, Fernandes CJ, Johnson A, Lally KP, Slavotinek A, Danhaive O, Schaible T, Cheung SW, Rauen Ka, Tonk VS, Tibboel D, de Klein A, Scott Da. Genomic alterations that contribute to the development of isolated and non-isolated congenital diaphragmatic hernia. *J Med Genet*. 2011; 48:299–307. [10.1136/jmg.2011.089680](https://doi.org/10.1136/jmg.2011.089680) [PubMed: 21525063]
- Wilm B, Ipenberg A, Hastie ND, Burch JBE, Bader DM. The serosal mesothelium is a major source of smooth muscle cells of the gut vasculature. *Development*. 2005; 132:5317–5328. [10.1242/dev.02141](https://doi.org/10.1242/dev.02141) [PubMed: 16284122]
- Yin Y, Wang F, Ornitz DM. Mesothelial- and epithelial-derived FGF9 have distinct functions in the regulation of lung development. *Development*. 2011; 138:3169–3177. [10.1242/dev.065110](https://doi.org/10.1242/dev.065110) [PubMed: 21750028]
- You LR, Takamoto N, Yu CT, Tanaka T, Kodama T, Demayo FJ, Tsai SY, Tsai MJ. Mouse lacking COUP-TFII as an animal model of Bochdalek-type congenital diaphragmatic hernia. *Proc Natl Acad Sci U S A*. 2005; 102:16351–16356. [10.1073/pnas.0507832102](https://doi.org/10.1073/pnas.0507832102) [PubMed: 16251273]
- Yuan W, Rao Y, Babiuk RP, Greer JJ, Wu JY, Ornitz DM. A genetic model for a central (septum transversum) congenital diaphragmatic hernia in mice lacking Slit3. *Proc Natl Acad Sci U S A*. 2003; 100:5217–5222. [10.1073/pnas.0730709100](https://doi.org/10.1073/pnas.0730709100) [PubMed: 12702769]
- Zeisberg M, Neilson EG. Biomarkers for epithelial-mesenchymal transitions. *J Clin Invest*. 2009; 119:1429–1437. [10.1172/JCI36183](https://doi.org/10.1172/JCI36183) [PubMed: 19487819]
- Zhang B, Xiao W, Qiu H, Zhang F, Moniz Ha, Jaworski A, Condac E, Gutierrez-Sanchez G, Heiss C, Clugston RD, Azadi P, Greer JJ, Bergmann C, Moremen KW, Li D, Linhardt RJ, Esko JD, Wang L. Heparan sulfate deficiency disrupts developmental angiogenesis and causes congenital diaphragmatic hernia. *J Clin Invest*. 2014; 124:209–221. [10.1172/JCI71090](https://doi.org/10.1172/JCI71090) [PubMed: 24355925]
- Zhou B, Honor LB, He H, Ma Q, Oh JH, Butterfield C, Lin RZ, Melero-Martin JM, Dolmatova E, Duffy HS, von Gise A, Zhou P, Hu YW, Wang G, Zhang B, Wang L, Hall JL, Moses MA, McGowan FX, Pu WT. Adult mouse epicardium modulates myocardial injury by secreting non-cell-autonomous factors. *J Clin Invest*. 2011; 121:1894–1904. [10.1172/JCI45529](https://doi.org/10.1172/JCI45529) [PubMed: 21505261]
- Zhou B, Ma Q, Rajagopal S, Wu SM, Domian I, Rivera-Feliciano J, Jiang D, von Gise A, Ikeda S, Chien KR, Pu WT. Epicardial progenitors contribute to the cardiomyocyte lineage in the developing heart. *Nature*. 2008; 454:109–113. [10.1038/nature07060](https://doi.org/10.1038/nature07060) [PubMed: 18568026]
- Zhou B, Pu WT. Genetic Cre-loxP assessment of epicardial cell fate using Wt1-Driven cre alleles. *Circ Res*. 2012; 111:e276–e280. [10.1161/CIRCRESAHA.112.275784](https://doi.org/10.1161/CIRCRESAHA.112.275784) [PubMed: 23139287]

### Highlights

- An inducible *Wt1<sup>CreERT2</sup>* mouse CDH model using  $\beta$ -catenin floxed mice was developed.
- *Wt1* regulates  $\beta$ -catenin expression in the mesothelium of the developing diaphragm.
- $\beta$ -catenin in *Wt1*<sup>+</sup> cells is necessary and sufficient to drive diaphragm development.
- Essential functions of  $\beta$ -catenin occur at a specific time in diaphragm development.
- *Wt1*, but not  $\beta$ -catenin, critically regulates diaphragm mesothelium maturation.



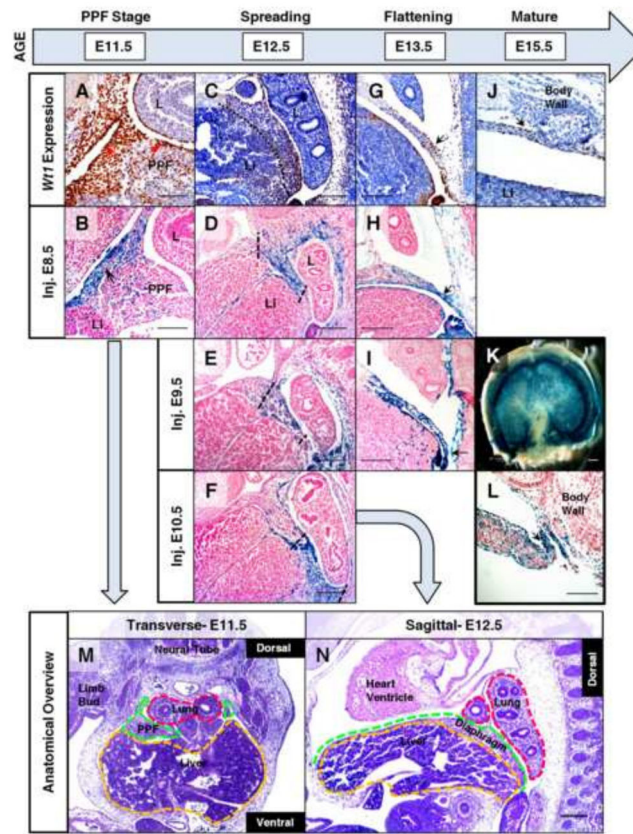


**Fig. 1.**

*Wt1* contribution shifts in developing diaphragm mesothelium and mesenchyme in a time-dependent manner. Immunohistochemistry (A, C, G, J) was performed on tissue sections from wildtype mice at E11.5 to E15.5 to detect *Wt1* protein localization in the developing diaphragm. Fate mapping was performed using whole-mount (B, D–F, H, K, L), or cryosectioned (I), X-gal stained *Wt1<sup>CreERT2</sup>;R26RlacZ* embryos harvested at E11.5 to E15.5 with recombination induced by tamoxifen injection at E8.5 (B, D, H), E9.5 (E, I), or E10.5 (F, K, L). *Wt1* protein and *Wt1*-derived cells were localized to mesothelium of the PPF (arrows) in transverse sections at E11.5 (A, B). Injecting at different time points resulted in restricted patterns of *lacZ* expression in sagittal sections at E12.5 (dotted lines) (D–F). Arrows indicate concentrated regions of *Wt1* protein and *Wt1* fate-mapped cells at E13.5 (G–I) and E15.5 (J–L). A whole X-gal stained diaphragm (K) at E15.5, injected at E10.5, is shown with a corresponding sagittal section (L). Low magnification H & E stained sections of representative wildtype embryos at E11.5 (M) and E12.5 (N) have relevant tissues and orientation labeled which is maintained throughout subsequent figures. Abbreviations: L, lung; Li, liver; PPF, pleuroperitoneal fold. The liver/diaphragm boundary is represented by a dotted line (C) where necessary. Scale bars: A, B, J, and L, 100  $\mu$ m; C–I, M and N, 200  $\mu$ m; K, 1 mm.

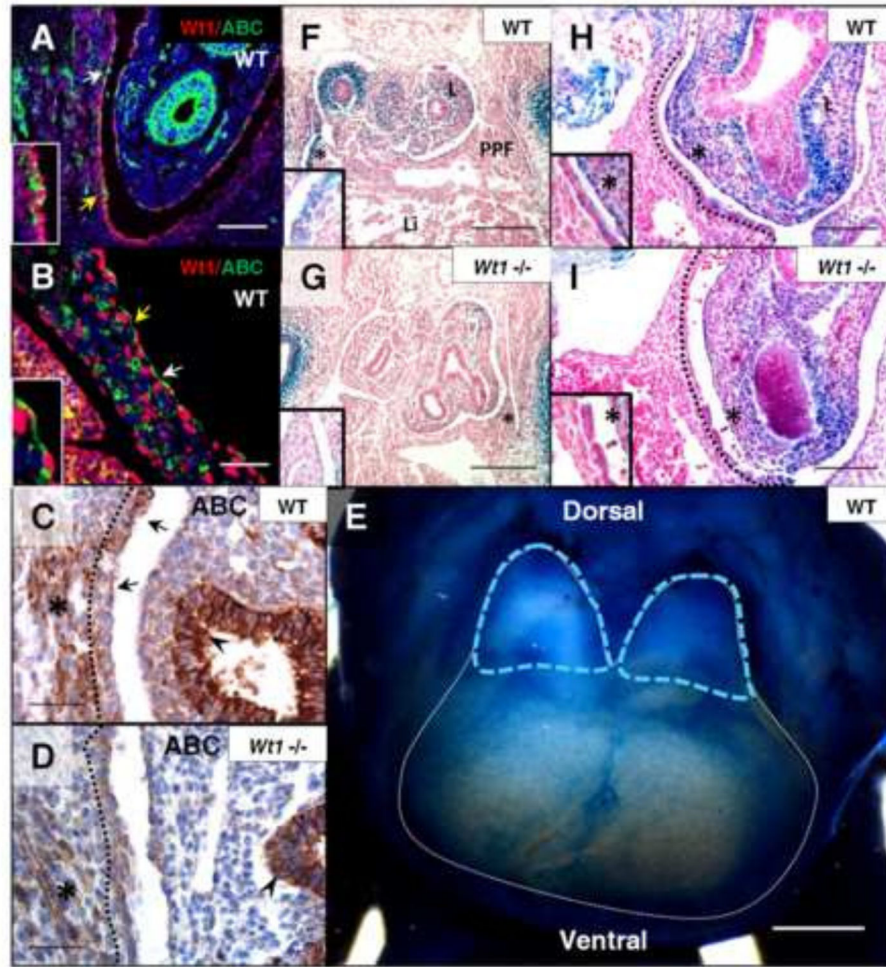


**Fig. 2.** Loss of *Wt1* results in reduced  $\beta$ -catenin expression in posterior diaphragm mesothelium. *Wt1*/Active  $\beta$ -catenin co-immunofluorescence was performed on sagittal sections of wildtype embryos at E12.5 (A) and E13.5 (B). *Wt1* nuclear protein corresponds to regions of Active  $\beta$ -catenin staining in the mesothelial cell cytoplasm (arrows). Insets are cropped images of regions with yellow arrows. Active  $\beta$ -catenin immunohistochemistry (C, D) of E13.5 *Wt1*<sup>GFPCre</sup> wildtype and mutant (*Wt1*<sup>GFPCre/GFPCre</sup>) diaphragms labels regions of mesothelium (dotted line), indicated by arrows, as well as diaphragm muscle (asterisks) and lung epithelium (arrowheads). E12.5 whole mount X-gal stained *Axin2*<sup>lacZ</sup> wildtype embryonic diaphragm (E) has been outlined in white, with blue dotted lines marking late PPF, dorsal and ventral sides are indicated. *Axin2*<sup>lacZ</sup>;*Wt1*<sup>GFPCre</sup> embryos were harvested at E11.5 (F–I) and sectioned in transverse (F, G) and sagittal (H, I) orientation following whole mount X-gal staining. Insets are high magnification of region marked by asterisk. Abbreviations: ABC, Active  $\beta$ -catenin; L, lung; Li, liver; PPF, pleuroperitoneal fold. Scale bars: A, B, H and I, 100  $\mu$ m; C and D, 50  $\mu$ m; F and G, 200  $\mu$ m; E, 0.5 mm.

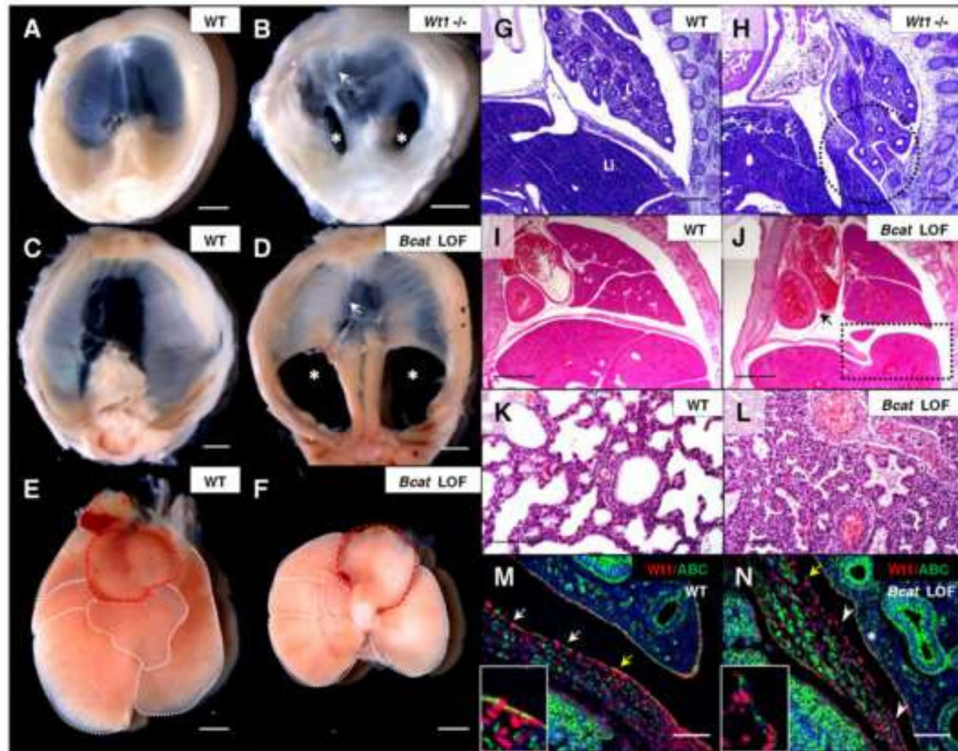


**Fig. 3.** *Wt1*-conditional loss of  $\beta$ -catenin leads to development of bilateral CDH similar to *Wt1*-null embryos. *Wt1*<sup>GFP<sup>Cre</sup></sup> homozygous mutants were collected at E15.5 (A, B) and dissected to observe gross morphology compared to age-matched controls. H&E stained *Wt1*<sup>GFP<sup>Cre</sup></sup> sagittal sections at E14.5 (G, H) have the *Wt1* mutant diaphragm defect with lung herniation circled. *Wt1*<sup>CreERT2</sup>;*Bcat*<sup>flx</sup> embryos, with Cre recombination induced at E10.5 by tamoxifen injection, were dissected at P0 with age-matched controls to view diaphragm (C, D) and cardiopulmonary (E, F) morphology. The heart (outlined in red) and lungs are displaced, though the correct number of lobes of the lung (outlined in white) are present. Bilateral posterior diaphragm defects (asterisks) and the myotendonous junction at the central tendon (arrows), defective only in the *Wt1* null, are labeled in mutant diaphragms (B, D). H&E stained *Wt1*<sup>CreERT2</sup>;*Bcat*<sup>flx</sup> sagittal sections at E16.5 (I, J) show liver herniation through the posterior defect (box) and associated lung and heart compression (arrow), also shown in high magnification of lung sections at P0 (K, L). *Wt1*/Active  $\beta$ -catenin co-immunofluorescence of E13.5 *Wt1*<sup>CreERT2</sup>;*Bcat*<sup>flx</sup> sagittal sections (M, N) confirmed substantial loss of Active  $\beta$ -catenin in mutant mesothelium in the posterior diaphragm (arrowheads, N). Regions of *Wt1*/Active  $\beta$ -catenin overlap (arrows, M) are present in the wildtype, whereas in the mutant, *Wt1*-positive cells no longer overlap with few remaining Active  $\beta$ -catenin-positive cells (yellow arrow, N). Insets are cropped images of regions labeled by yellow arrows. Asterisk denotes retention of positive Active  $\beta$ -catenin staining in mutant lung mesothelium (N). Whole mature diaphragms are pictured with the dorsal side at the bottom (A–D). Abbreviations: L, lung; Li, liver. Scale bars: A–F, I and J, 1 mm; G and H, 200  $\mu$ m; K–N, 100  $\mu$ m.

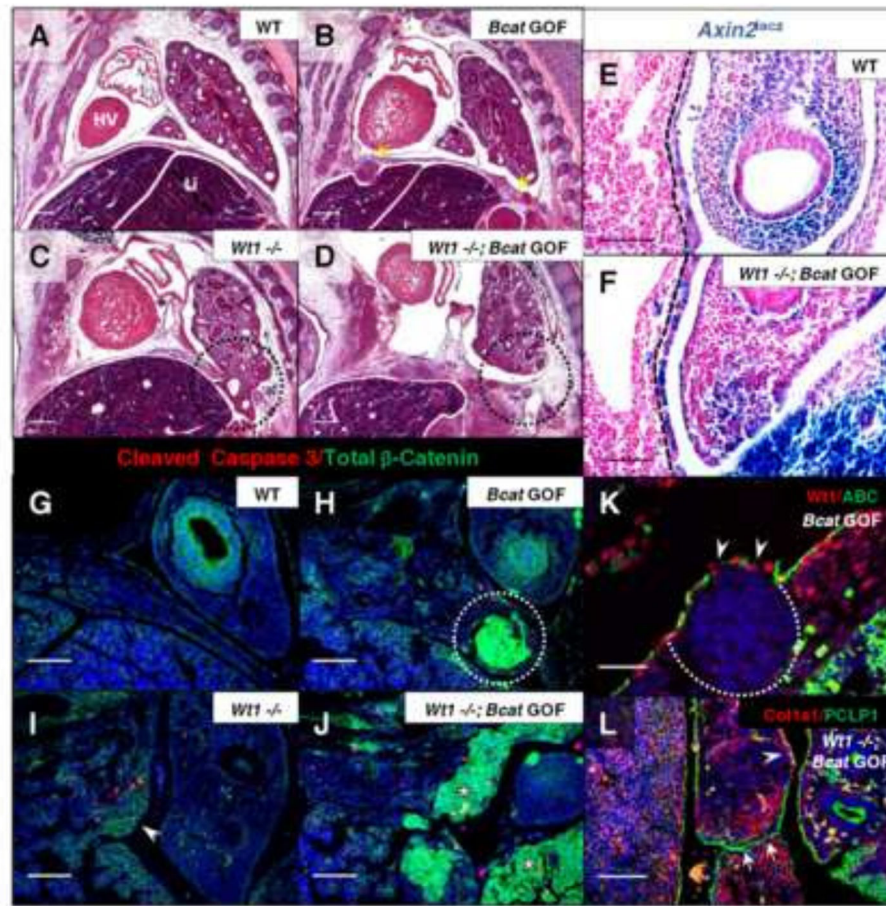


**Fig. 4.**

Induction of constitutively active  $\beta$ -catenin in the *Wt1* lineage results in mesenchymal overgrowth sufficient to close *Wt1* null diaphragm defects. H&E stained sagittal sections of *Wt1<sup>CreERT2</sup>;Bcat<sup>ex3fx</sup>* embryos, injected with tamoxifen at E10.5 and harvested at E13.5 (A–D), illustrate phenotypes of single and double mutants compared to wildtype. Yellow arrows indicate where nodules have formed in the gain-of-function diaphragm (B) and the affected region of the posterior diaphragm in the *Wt1* single and double mutants is circled (C, D). *Wt1<sup>CreERT2</sup>;Bcat<sup>ex3fx</sup>;Axin2<sup>lacZ</sup>* embryos at E11.5 were whole-mount X-gal stained and sectioned sagittally (E, F). The positively stained posterior diaphragm mesothelium is demarcated by dotted lines. Co-immunofluorescence of Total  $\beta$ -catenin and Cleaved Caspase 3 was carried out on *Wt1<sup>CreERT2</sup>;Bcat<sup>ex3fx</sup>* E12.5 paraffin sections (G–J). Constitutively active  $\beta$ -catenin is shown in nodules (circle, H) and adjacent to *Wt1* null diaphragm defects (asterisks, J). Presence of only membranous total  $\beta$ -catenin is indicated in single *Wt1* null (arrowhead, I). Co-immunofluorescence was carried out at E13.5 of *Wt1*/Active  $\beta$ -catenin in diaphragm nodules in  $\beta$ -catenin gain-of-function (K) and Collagen I $\alpha$ 1/Podocalyxin (PCLP1) in *Wt1<sup>CreERT2</sup>;Bcat<sup>ex3fx</sup>* double mutant (L) posterior diaphragms. Dotted line outlines the nuclei-dense growth and arrowheads indicate loss of phosphorylation site-specific antibody staining where  $\beta$ -catenin exon 3 has been excised (K). Arrows indicate mesothelial fusion (L), where diaphragm tissue has grown together

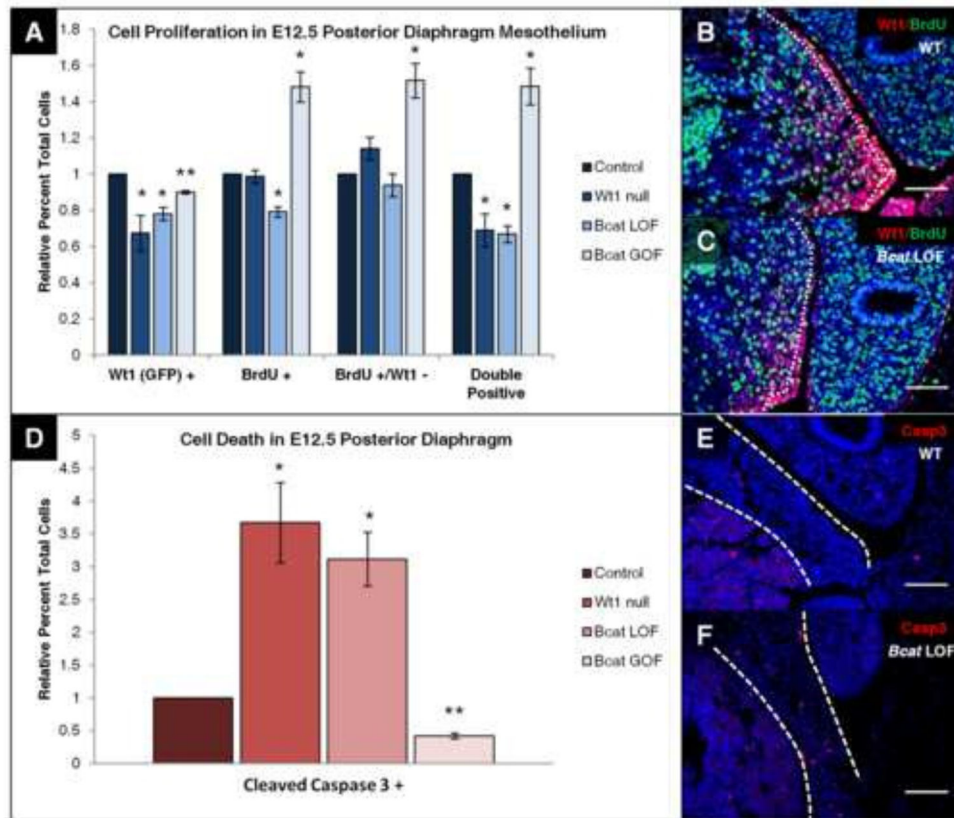
after the initial *Wt1* defect was already formed. Arrowhead labels a region of wildtype localization of *Col1a1*. Abbreviations: HV, Heart Ventricle; L, lung; Li, liver. Scale bars: A–D, 200  $\mu\text{m}$ ; E–J, and L, 100  $\mu\text{m}$ ; K, 50  $\mu\text{m}$ .

Author Manuscript

Author Manuscript

Author Manuscript

Author Manuscript

**Fig. 5.**

*Wt1* and  $\beta$ -catenin regulate cell proliferation and cell death in the posterior diaphragm. Littermate pairs of E12.5 *Wt1* null (*Wt1*<sup>GFP<sup>Cre</sup>/GFP<sup>Cre</sup>),  $\beta$ -catenin loss-of-function (*Wt1*<sup>CreERT2/+</sup>; *Bcat*<sup>fx/fx</sup>), and  $\beta$ -catenin gain-of-function (*Wt1*<sup>CreERT2/+</sup>; *Bcat*<sup>ex3fx/ex3fx</sup>), embryonic sections were co-stained for *Wt1* (or GFP) and BrdU to assay cell proliferation (A). Means of the relative percent of total single positive cells and double positive cells in the posterior diaphragm mesothelium were plotted with standard error of mean. Representative sections (B, C) are shown where dotted lines indicate the mesothelium. E12.5 *Wt1* null,  $\beta$ -catenin loss-of-function, and  $\beta$ -catenin gain-of-function embryonic sections were also stained for Cleaved Caspase 3 to analyze cell death in the posterior diaphragm (D). Means of the relative percent of total Cleaved Caspase 3 positive cells were plotted with standard error of mean. Representative sections (E, F) have dotted lines indicating the domain of the posterior diaphragm in which cells were counted.  $N=3$  for both experiments. All values were compared to normalized littermate Cre-negative wildtype control (for  $\beta$ -catenin mice) or *Wt1*<sup>GFP<sup>Cre</sup></sup> heterozygous control (\* $P<0.05$ , \*\* $P<0.01$ ,  $t$ -test). Scale bar: B–F, 100  $\mu$ m.</sup>

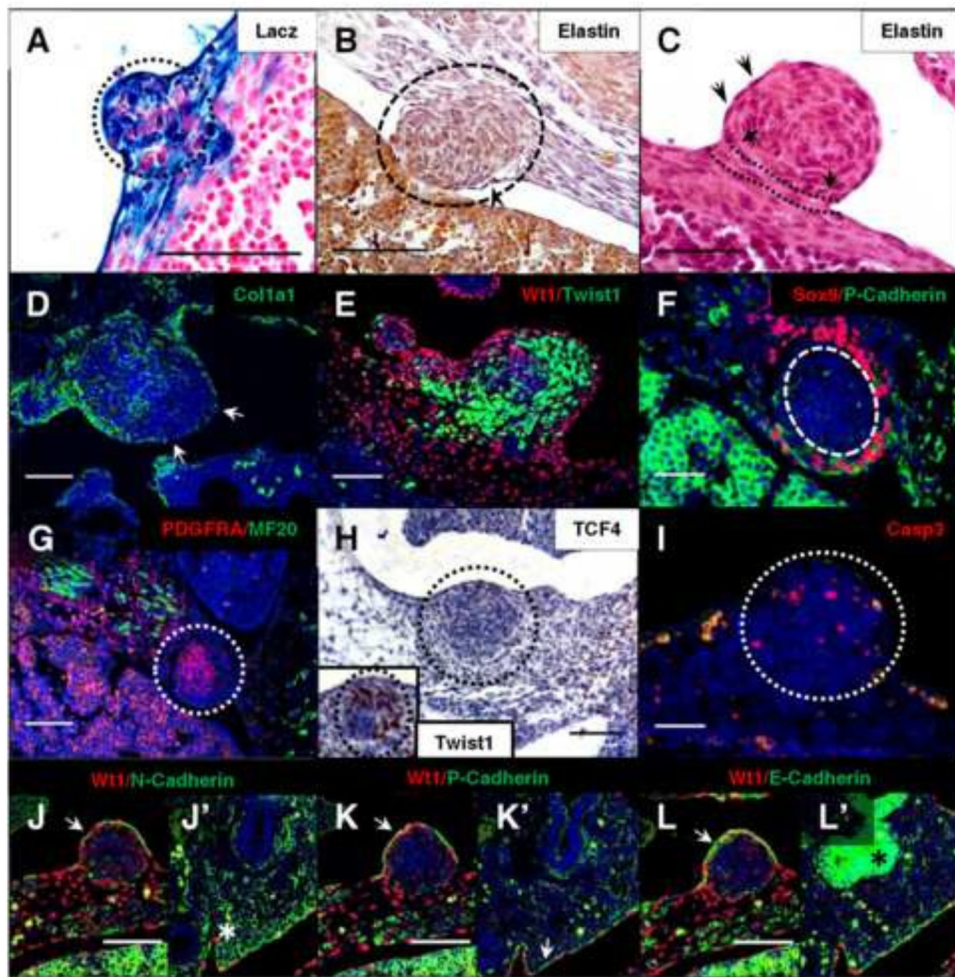


**Fig. 6.** Activation of  $\beta$ -catenin in *Wt1*-expressing cells amplifies a population of undifferentiated mesenchymal cells. *Wt1<sup>CreERT2</sup>;Bcat<sup>ex3fx</sup>* embryos containing the *R26RlacZ* reporter (A) were analyzed at E13.5 by sectioning following whole mount X-gal staining. Nodules in *Wt1<sup>CreERT2</sup>;Bcat<sup>ex3fx</sup>* diaphragms were further characterized by histological staining of elastin fibers, which are apparent by regions of black/dark purple staining (arrowheads) of the mesothelial cell periphery at E13.5 (B) and E12.5 (C). Arrows and dotted lines (C) indicate an intact sub-mesothelial layer beneath the nodule, where pink eosin-stained collagen fibers could not be infiltrated. Collagen1a1 staining of the basement membrane (D) at E13.5 is absent in regions of the nodule mesothelium (arrows). At E13.5 (E) and E12.5 (F, G), early mesenchymal markers Twist1, Sox9, and Pdgfra were detected through co-immunofluorescence with mesothelial proteins Wt1 (E) and P-Cadherin (F), as well as muscle marker MF20 (Myosin) (G). *Wt1<sup>CreERT2</sup>;Bcat<sup>ex3fx</sup>* E13.5 diaphragm nodules were immunostained to detect connective tissue marker TCF4 (H) and Twist1 (inset, H) in serial sections of the same embryo, as well as cell death marker Cleaved Caspase 3 (I). At E13.5, mesothelial proteins N-Cadherin (J), P-Cadherin (K), and E-Cadherin (L) were detected by co-immunofluorescence with Wt1. Corresponding positive regions of nodule mesothelium are indicated by arrows (J, K, L). Regions of known positivity in the lung are labeled with

asterisks (J', L') or an arrow (K'). All nodules are outlined with circles where necessary.  
Scale bars: A, B, D, E, G, and J–L, 100  $\mu\text{m}$ ; C, F, and I, 50  $\mu\text{m}$ ; H, 200  $\mu\text{m}$ .

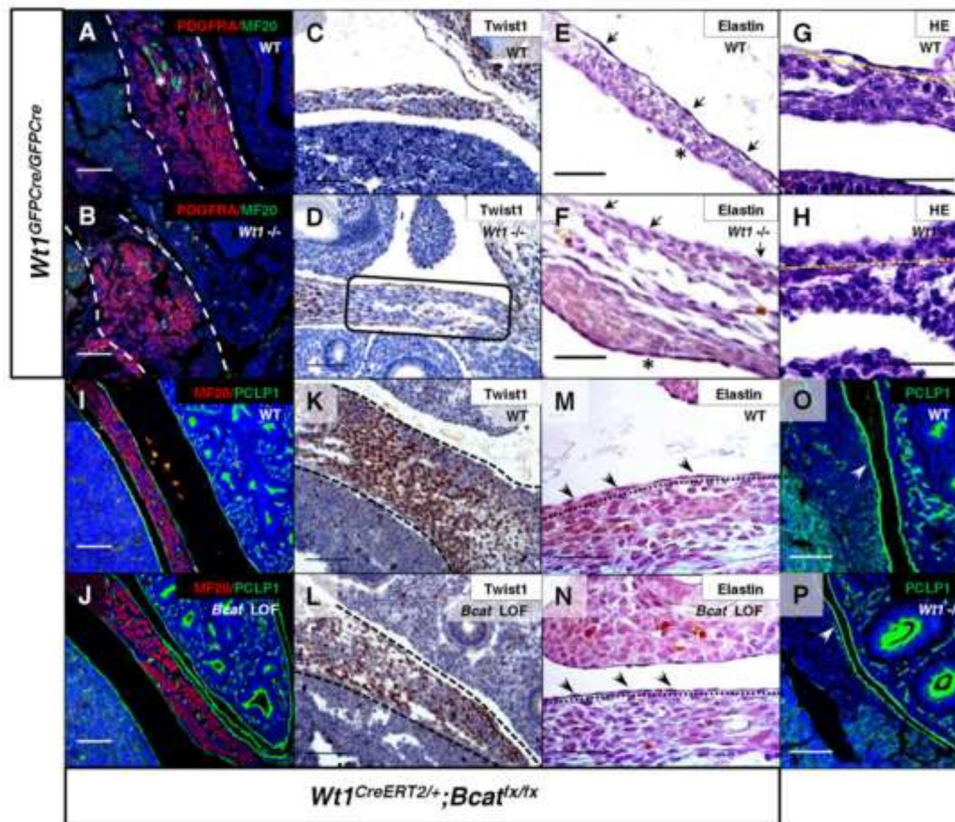
Author Manuscript

Author Manuscript

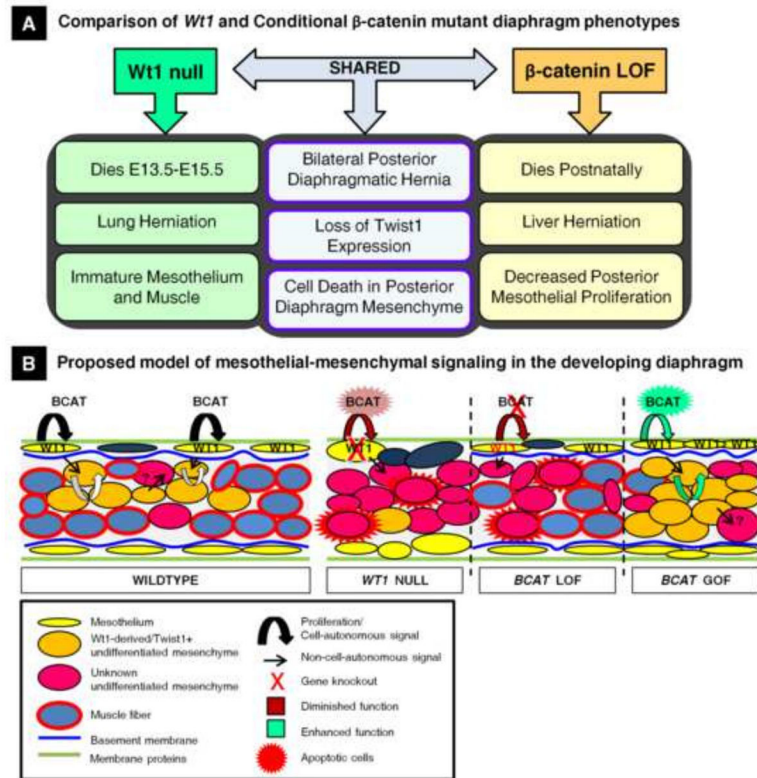
Author Manuscript

Author Manuscript





**Fig. 7.** *Wt1* and  $\beta$ -catenin are necessary for proper posterior diaphragm patterning. Differentiation in the posterior diaphragm of *Wt1*<sup>GFP</sup>Cre null embryos was assayed by immunostaining at E12.5 for Pdgfra and MF20-positive muscle (A, B), and at E13.5 for Twist1 (C, D). An asterisk labels a region of positive muscle staining (A) and a box (D) indicates differential Twist1 staining in a region of the posterior diaphragm adjacent to site of defect (evident by lung herniation) (D). Mesothelial cell differentiation was assayed by histology of elastin fibers at E14.5 (E, F) and H&E staining at E13.5 for analysis of morphology (G, H). Note positively stained elastin fibers are still seen in mesothelium on abdominal surface (asterisk). Arrows (E, F) indicate presence and absence of elastin in the wildtype and mutant, respectively, and yellow lines (G, H) are drawn below the mesothelium. Co-immunofluorescence of Myosin (MF20) and Podocalyxin (PCLP1) (I, J) performed on E13.5 *Wt1*<sup>CreERT2/+</sup>;*Bcat*<sup>lox</sup> sagittal sections showed no difference from wildtype. Further immunohistochemistry (K, L) revealed loss of Twist1 in diaphragm mesenchyme (within dotted lines). Analysis of  $\beta$ -catenin loss-of-function diaphragms at E13.5 by histology for elastin (M, N) also shows no change. *Wt1*<sup>GFP</sup>Cre mutants at E12.5 demonstrated wildtype levels of mesothelial PCLP1 (O, P) detected by immunofluorescence in the posterior diaphragm. Single lines label the elastin-stained mesothelium (arrows, M and N) and white arrows indicate PCLP1-positive mesothelium (O, P). Scale bars: A–D, I–L, O and P, 100  $\mu$ m; E–H, M and N, 50  $\mu$ m.

**Fig. 8.**

A model for *Wt1* and  $\beta$ -catenin regulation of mesothelial maintenance signaling necessary for proper differentiation of the posterior diaphragm mesenchyme. (A) A summary of the similarities and differences seen in the *Wt1* null and *Wt1*<sup>CreERT2</sup>;*Bcat*<sup>flx</sup> mutant diaphragm phenotypes. (B) A schematic summarizes our findings comparing the dynamics of diaphragm differentiation in *Wt1* null,  $\beta$ -catenin loss-of-function and gain-of-function embryos and proposes a mechanism that, when defective, results in the phenotypes observed.